MCB
Journals.ASM.org

Histone Deacetylase 10 Regulates the Cell Cycle G_2/M Phase Transition via a Novel Let-7–HMGA2–Cyclin A2 Pathway

Yixuan Li, Lirong Peng, Edward Seto

Department of Molecular Oncology, Moffitt Cancer Center, Tampa, Florida, USA

Histone deacetylase (HDAC) inhibition leads to cell cycle arrest in G_1 and G_2, suggesting HDACs as therapeutic targets for cancer and diseases linked to abnormal cell growth and proliferation. Many HDACs are transcriptional repressors. Some may alter cell cycle progression by deacetylating histones and repressing transcription of key cell cycle regulatory genes. Here, we report that HDAC10 regulates the cell cycle via modulation of cyclin A2 expression, and cyclin A2 overexpression rescues HDAC10 knockdown-induced G_2/M transition arrest. HDAC10 regulates cyclin A2 expression by deacetylating histones near the *let-7* promoter, thereby repressing transcription. In *HDAC10* knockdown cells, *let-7f* and microRNA 98 (miR-98) were upregulated and the *let-7* family target, *HMGA2*, was downregulated. HMGA2 loss resulted in enrichment of the transcriptional repressor E4F at the cyclin A2 promoter. These findings support a role for HDACs in cell cycle regulation, reveal a novel mechanism of HDAC10 action, and extend the potential of HDACs as targets in diseases of cell cycle dysregulation.

Histone function is modulated by several posttranslational modifications, including reversible acetylation of the N-terminal ε-group of lysines on histones (1). Histone acetylation is tightly controlled by a balance between the opposing activities of histone acetyltransferases and histone deacetylases (HDACs). Acetylation of histone core molecules modulates chromatin structure and gene expression (2). The human HDAC family includes 18 members grouped into four classes. Class I HDACs, orthologs of *Saccharomyces cerevisiae* RPD3, are comprised of HDAC1, -2, -3, and -8. Class II, similar to yeast HDA1, has two subclasses: IIa (HDAC4, -5, -6, -7, and -9) and IIb (HDAC6 and -10). Class III, related to yeast SIR2, consists of seven sirtuins, which require NAD^+ for activity. Class IV contains only HDAC11, which shows limited homologies to class I and II enzymes. Whereas class III HDACs are inhibited by nicotinamide, class I and II HDACs are dependent on Zn^{2+} for deacetylase activity. The class IIb HDAC6 and HDAC10 are specifically sensitive to hydroxamate-type inhibitors (3), such as trichostatin A (TSA) and suberoylanilide hydroxamic acid (SAHA). Most hydroxamate inhibitors are nonselective, with the exception of tubacin and tabastatin A, which are selective for HDAC6 (4, 5). Another hydroxamate compound, bufexamac, also has been identified as a novel class IIb inhibitor that specifically inhibits HDAC6 at lower doses (3, 6). In addition, the cellular acetylome regulated by HDAC6 correlated with the profile observed after bufexamac treatment (6). However, the effect and mechanism of bufexamac on HDAC10 have not yet been well-studied. Thus, identification of the catalytic structure and mechanism of action of HDAC10 might inform the development of a selective inhibitor in future research.

HDACs play important roles in the regulation of the cell cycle, apoptosis, stress responses, and DNA repair, indicating that they are key regulators of normal cell growth and proliferation (2, 7); HDAC inhibitors have been shown to have antiproliferative effects (8, 9). For example, deletion of HDAC1 and -2 results in a strong proliferation block followed by apoptosis. HDAC1 and -2 directly bind to the promoters of the $p21^{WAF1/CIP1}$ (10–12), $p27^{KIP1}$ (8, 10), and $p57^{KIP2}$ (12) genes and negatively regulate their expression. Loss of HDAC1 and -2 induces expression of these cyclin-dependent kinase (CDK) inhibitors, leading to a cell cycle block in G_1. HDAC1 knockdown in tumor cells also impairs the G_2/M transition and inhibits cell growth, as evidenced by a reduction of mitotic cells and an increased percentage of apoptotic cells (13). Inhibition of HDACs also causes cell cycle arrest at the G_2/M boundary in a variety of tumor cell lines (14–18).

In addition to transcriptional repression of cell cycle-related genes, HDACs might also regulate cell cycle progression in a transcription-independent manner. HDAC3 is a critical, transcription-independent regulator of mitosis that forms a complex with AKAP95 and HA95. During mitosis, AKAP95/HA95 recruit HDAC3 along with Aurora B. Subsequently, HDAC3-mediated histone deacetylation facilitates maximal phosphorylation of histone H3 on Ser10 by Aurora B, leading to HP1β dissociation from mitotic chromosomes. The HDAC3-AKAP95/HA95-Aurora B pathway is required for normal mitotic progression (19). HDAC3 also directly interacts with cyclin A and regulates cyclin A stability by modulating its acetylation status. An abrupt loss of HDAC3 at metaphase facilitates cyclin A acetylation by PCAF/GCN5, which target cyclin A for degradation. Because cyclin A is crucial for S-phase progression and entry into mitosis, HDAC3 knockdown causes cell accumulation in the S and G_2/M phases (20).

HDAC10 is a class IIb HDAC that was first discovered based on sequence homology to other class II HDACs (21–23). Class IIb HDACs are structurally distinct from class I and class IIa HDACs: HDAC6 possesses two homologous active domains, and HDAC10

Received 17 April 2015 **Returned for modification** 11 May 2015
Accepted 30 July 2015

Accepted manuscript posted online 3 August 2015

Citation Li Y, Peng L, Seto E. 2015. Histone deacetylase 10 regulates the cell cycle G_2/M phase transition via a novel Let-7–HMGA2–cyclin A2 pathway. Mol Cell Biol 35:3547–3565. doi:10.1128/MCB.00400-15.

Address correspondence to Edward Seto, ed.seto@moffitt.org.

Supplemental material for this article may be found at http://dx.doi.org/10.1128/MCB.00400-15.

doi:10.1128/MCB.00400-15

possesses one catalytic domain and one additional leucine-rich incomplete catalytic domain (21–24). Unlike HDAC6, which is located chiefly in the cytoplasm, HDAC10 resides in both the nucleus and the cytoplasm. In the nucleus, HDAC10 deacetylates histones and represses transcription when tethered to a target promoter (21–24). HDAC10 is involved in transcriptional downregulation of TXNIP, leading to altered signaling in response to reactive oxygen species and apoptosis in human gastric cancer cells (25). HDAC10 binds to the *MMP2* and *-9* promoters, reduces histone acetylation, and inhibits transcription in cervical cancer cells (26). In addition to transcriptional regulation, HDAC10 might also target nonhistone proteins. HDAC10, together with HDAC1 and -3, and SIRT1 and -2, regulated the 3′-end processing machinery by modulating deacetylation of CFIm25 and PAP, ultimately affecting the CFIm25-PAP interaction and PAP localization (27). In neuroblastoma cells, HDAC10 promoted autophagy-mediated survival and protected cells from cytotoxic agents by direct interaction with, and deacetylation of, Hsc70/Hsp70 (28).

Previous reports indicated that HDAC10 expression was significantly decreased in lung cancer, gastric cancer, and adrenocortical carcinoma tissues, and this may be a reliable predictor of a poor prognosis in patients with these cancers (29–31). In contrast, for neuroblastomas, medulloblastomas, and chronic lymphocytic leukemias, HDAC10 expression was significantly increased in tumor tissues and correlated with poor survival (28, 32). Although HDAC10 is ubiquitously expressed (21, 23, 24), its role in cell cycle regulation is largely unknown. We hypothesize that HDAC10 regulates the cell cycle via modulation of cyclin A. Therefore, we examined the role of HDAC10 in cell cycle regulation by using a panel of human non-small cell lung cancer (NSCLC) cell lines. HDAC10 knockdown widely suppressed cell proliferation by inhibiting premature entry into mitosis. Loss of cyclin A2 in *HDAC10* knockdown cells contributed to G_2/M arrest. The effect of HDAC10 on cyclin A2 transcription was dependent on *let-7* and *HMGA2*.

MATERIALS AND METHODS

Cell lines and culture. HEK 293T, HeLa, LL24, the NSCLC cell lines H1299, H441, H23, H157, H2122, H358, A549, PC9, H1975, H322, H292, H460, H522, and H661, and ADLC-5M2 cells were grown in Dulbecco's modified Eagle medium (DMEM) with 10% fetal bovine serum (FBS) and 1% penicillin-streptomycin at 37°C in a humidified atmosphere of 5% CO_2.

MEF isolation and culture. Mouse embryonic fibroblasts (MEFs) were isolated and maintained as described previously (33). Briefly, embryos (embryonic day 13 [E13] to E14) were dissected from euthanized pregnant females and washed with sterile phosphate-buffered saline (PBS). Heads were removed for isolation of genomic DNA and genotyping by PCR. The rest of each embryo was cut into pieces in a sterile dish and incubated with 1 ml 0.25% trypsin–EDTA at 37°C in a 5% CO_2 incubator for 15 min, with pipetting up and down several times every 5 min to break up tissue chunks. The trypsinized cells were then mixed with 10 ml DMEM–10% FBS and incubated at 37°C in a 5% CO_2 incubator. Viable MEFs were harvested at passage 2 (P2), stored in liquid nitrogen, and used between P3 and P7.

Plasmids and oligonucleotides. FLAG-tagged HDAC10 was the kind gift of X. J. Yang (21). DNA encoding full-length HDAC10 was subcloned into the EcoRI/KpnI site of pEGFP-C2, and the *HDAC10* short hairpin RNA (shRNA) resistance mutation was generated using the QuikChange multisite-directed mutagenesis kit (Stratagene, La Jolla, CA). pLenti-CMV-Neo-DEST/HDAC10 was constructed using the Gateway system (Life Technologies, Grand Island, NY). The HDAC10 H135A mutant was generated using the QuikChange site-directed mutagenesis kit (Stratagene) and confirmed by sequencing. The *HMGA2* full-length open reading frame (ORF) was inserted into the EcoRI/BamHI site of vector pcDNA3.1-FLAG. Cyclin A2 and *HMGA2* promoter reporter plasmids were generated by cloning into the KpnI/HindIII site of the pGL3-Basic vector using primers described in Table S1 in the supplemental material. CRE site mutations in the cyclin A2 gene (*CCNA2*) reporter plasmid CCNA2P-167 were produced by PCR overlap extension as described previously (34). Expression plasmids for human microRNA 98 (miR-98) and *let-7* were constructed by inserting a 700-bp human primary microRNA (pri-miRNA) into vector pcDNA3.1.

Lentiviral HDAC10 shRNA expression PLKO.1 plasmids (TRCN 0000004859, TRCN0000004860, and TRCN0000004861) were obtained from Thermo Fisher Scientific (Waltham, MA). The *HMGA2*-specific shRNA expression plasmid (TRCN0000021966) and *HDAC6* shRNA plasmid (TRC0000004839) were from Sigma-Aldrich (St. Louis, MO). PLKO.1-TRC scrambled control shRNA, pLKO.1-GFP shRNA plasmid, mouse Hmga2 3′ untranslated region (UTR) wild-type (wt) and m7 pIS1 luciferase plasmids, and venus-FLAG-tagged human cyclin A2 in pcDNA5/FRT/TO were from Addgene (Cambridge, MA). The cyclin A2 full-length ORF was subcloned into the EcoRI/XhoI site of vector pcDNA3.1-HA. V5-tagged E4F1 in vector pLX304 was from DNASU (Biodesign Institute at Arizona State University, Tempe, AZ). Specific *let-7f-5p* (AM10902) and miR-98-5p (AM10426) antisense oligonucleotides were from Applied Biosystems (Thermo Fisher Scientific). The E4F1-specific small interfering RNA (siRNA) duplex was synthesized by GE Dharmacon (Lafayette, CO) as described previously (35).

Preparation and transduction of shRNA. Lentivirus was prepared by transfecting HEK 293T cells with a scrambled control pLKO.1 TRC cloning vector or pLKO.1 expressing *HDAC10*-specific shRNA, together with packaging vectors. Lentivirus-transduced cells were selected for puromycin resistance, and the stably expressing cells were used for cell cycle experiments at passages P5 to P10.

Transduction of *HDAC10* knockout MEFs. Primary *HDAC10* knockout MEFs were transformed by infection with lentivirus encoding $NRas^{G12V}$. To perform the rescue experiments, the immortalized lines were transduced with lentiviral vectors expressing either wild-type HDAC10 or a catalytically inactive histidine-to-alanine (H135A) HDAC10 mutant and cultured with 0.5 mg/ml G418 for selection and maintenance of the stably expressing cells.

Cell cycle synchronization. Cells were synchronized in S phase by either double-thymidine block or 2 mM hydroxyurea treatment for 24 h. Cells were synchronized in M phase via 100 ng/ml nocodazole treatment for 16 h. For synchronization at the latest stages of G_2, cells were incubated in 10 μM RO-3306 for 20 h (36). MEFs were synchronized in G_1/S phase by serum deprivation (culture in DMEM– 0.1% FBS) for 48 h followed by stimulation with 10% FBS in the presence of 2 mM hydroxyurea for 24 h, followed by release. Cell cycle DNA distribution was confirmed by flow cytometry. The mitotic index (the percentage of cells in M phase) was based on the percentage of p-H3 (Ser10)-positive cells in the 4N population by flow cytometric analysis or on the fraction of cells with condensed chromosomes in a minimum of 500 cells scored by using image analysis.

Antibodies and reagents. Rabbit anti-HDAC10 (H3413) and mouse anti-FLAG M2 (F3165), anti-β-actin (A1978), anti-α-tubulin (T5168), anti-glyceraldehyde-3-phosphate dehydrogenase (anti-GAPDH; G8795), and antivinculin (V9131) antibodies were purchased from Sigma-Aldrich. Rabbit polyclonal anti-cyclin B1 (4138), anti-cyclin E2 (4132), anti-phospho-cdc2 (Tyr15; 9111), anti-phospho-CREB (Ser133; 9191), anti-phospho-histone H3 (Ser10; 3377), anti-histone H3 (4499), anti-acetyl-histone H3 (Lys9) (9649), anti-acetyl-histone H3 (Lys14) (7627), anti-acetyl-histone H3 (Lys18) (9675), anti-acetyl-histone H3 (Lys27) (4353), anti-acetyl-histone H4 (Lys5) (9672), anti-acetyl-lysine (9441), and anti-human cyclin A2 (4656) antibodies were from Cell Signaling Technology (Danvers, MA). Mouse monoclonal anti-cdc2 (p34), rabbit polyclonal anti-HDAC6 (H-300) and anti-lamin A (H-102), and anti-mouse cyclin A2 (C-19) antibodies

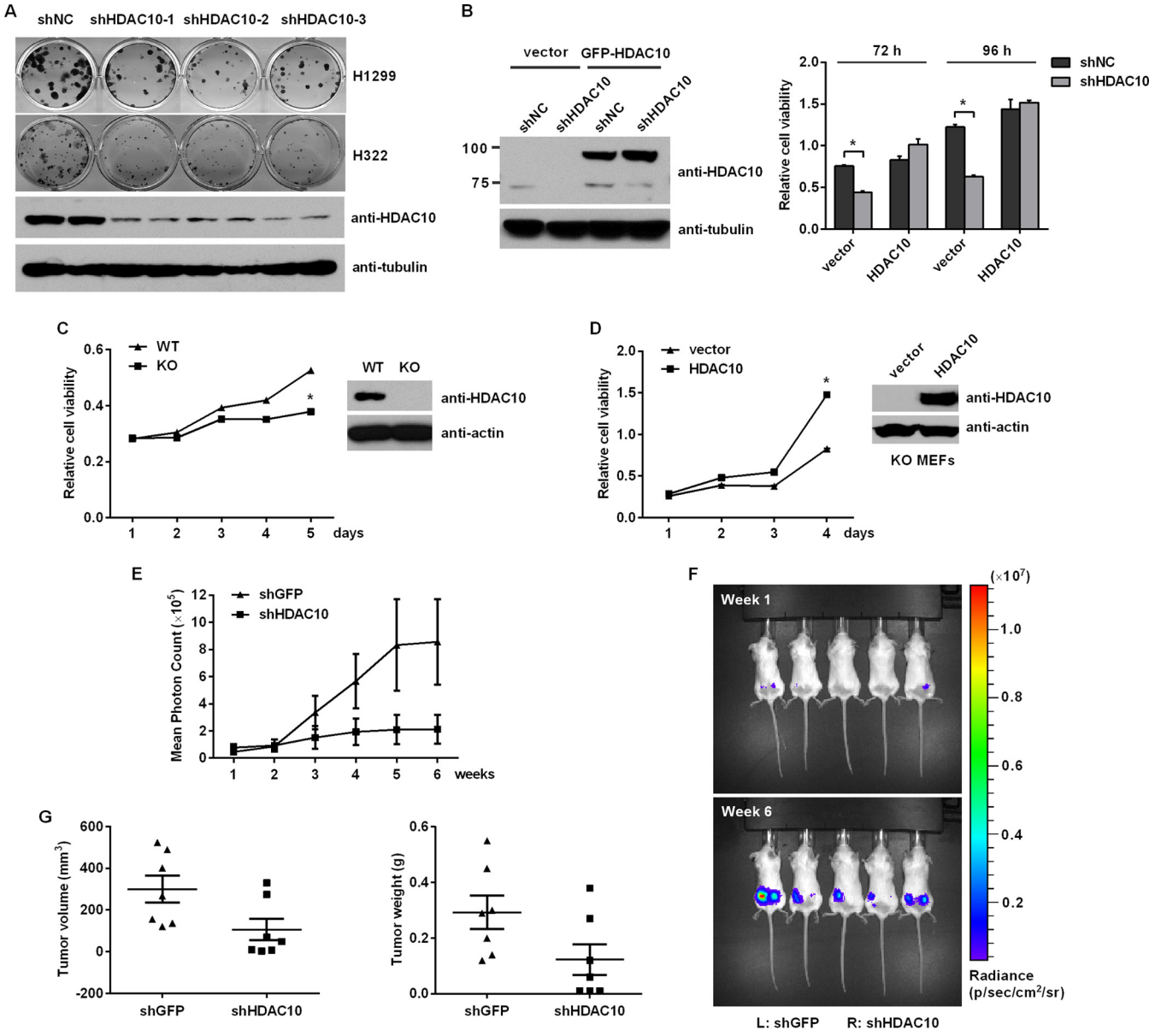

FIG 1 HDAC10 regulates cell proliferation *in vitro* and tumor growth *in vivo*. (A) Colony formation assay results (upper panels) of H1299 and H322 cells transduced with control shRNA (shNC) or the indicated shRNAs targeting HDAC10. (Lower panels) Western blot demonstration of HDAC10 knockdown. Tubulin served as the internal control. (B) Western analysis of HDAC10 expression in H1299 cells expressing the indicated shRNAs and then transiently transfected with vector alone or vector encoding GFP-tagged shRNA-resistant HDAC10. (Left) The upper bands represent GFP-tagged HDAC10, and lower bands represent endogenous HDAC10. (Right) Relative viability of cells at 72 h and 96 h posttransfection. (C and D) Relative viability of wt MEFs, *HDAC10* knockout (KO) MEFs, and *HDAC10* knockout MEFs transduced with lentiviral control or HDAC10 expression vectors at the indicated times (left) and by Western analysis (right). Values represent means ±standard deviations (SD). *, $P < 0.05$. (E) Tumor growth, based on bioluminescence imaging of luciferase activity of tumors at the indicated times after injection of A549-luc cells expressing control shGFP and shRNA targeting *HDAC10* into the left and right flanks, respectively, of female SCID-bg mice ($n = 7$). Values represent mean ± standard errors of the means (SEM). (F) Representative images of the mice described for panel E at weeks 1 and 6. (G) Volume (left) and weight (right) of tumors described for panel E at 7 weeks. Error bars indicate SEM.

were from Santa Cruz Biotechnology (Dallas, TX). Mouse monoclonal anti-V5 antibody (R960-25), Alexa Fluor 568-conjugated anti-mouse IgG (A-10037), Alexa Fluor 568-conjugated anti-rabbit IgG (A-11036), and Alexa Fluor 488-conjugated anti-rabbit IgG (A-31566) were obtained from Invitrogen (Thermo Fisher Scientific). Rabbit anti-HMGA2 antibody was from either Cell Signaling Technology (5269) or Active Motif (61041; Carlsbad, CA). Anti-acetyl-histone H3 (06-99) antibody was from EMD Millipore (Billerica, MA).

RO-3306 (SML0569), nocodazole (M1404), thymidine (T1895), hydroxyurea (H8627), TSA (T8552), bufexamac (B0760), tubacin (SML0065), tubastatin A (SML0044), and actinomycin D (A1410) were from Sigma-Aldrich. D-Luciferin potassium salt (LUCK-1G) used for *in vivo* imaging of luciferase was from Gold Biotechnology (Olivette, MO). The Click-iT 5-ethynyl-2′-deoxyuridine (EdU) Alexa Fluor 488 flow cytometry assay kit (C-10425) was from Invitrogen. A Dual-Luciferase reporter assay system (E1910) was from Promega (Madison, WI). Transfections

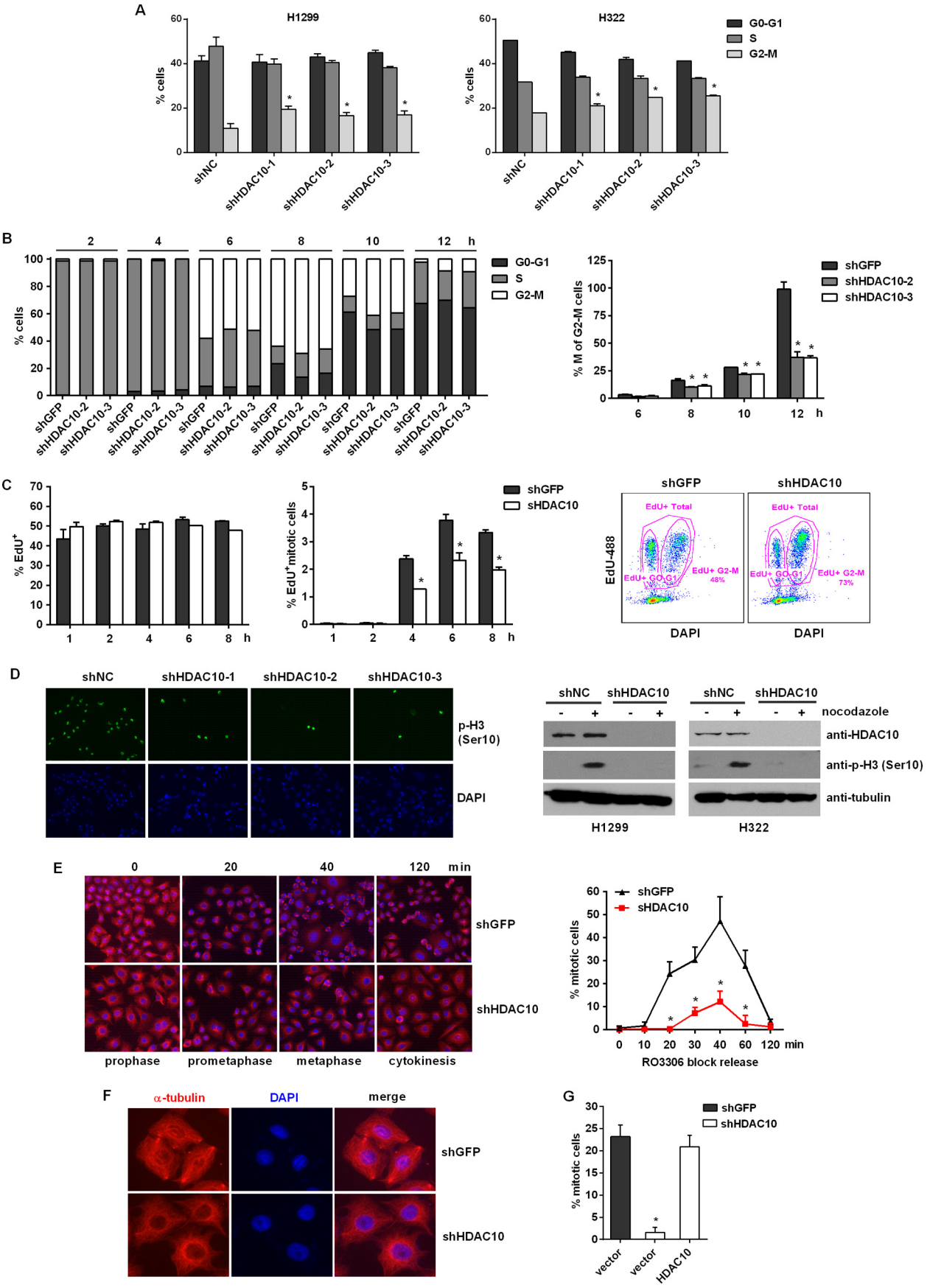
A
H1299
H322
% cells
G0-G1
S
G2-M
shNC
shHDAC10-1
shHDAC10-2
shHDAC10-3
B
% cells
% M of G2-M cells
shGFP
shHDAC10-2
shHDAC10-3
C
% EdU+
% EdU+mitotic cells
shGFP
sHDAC10
EdU-488
DAPI
EdU+ Total
EdU+ G0-G1
EdU+ G2-M
48%
73%
D
shNC
shHDAC10-1
shHDAC10-2
shHDAC10-3
p-H3 (Ser10)
DAPI
shNC
shHDAC10
nocodazole
anti-HDAC10
anti-p-H3 (Ser10)
anti-tubulin
H1299
H322
E
0
20
40
120 min
shGFP
shHDAC10
prophase
prometaphase
metaphase
cytokinesis
% mitotic cells
RO3306 block release
F
α-tubulin
DAPI
merge
shGFP
shHDAC10
G
% mitotic cells
shGFP
shHDAC10
vector
vector
HDAC10

of plasmids, siRNA, and oligonucleotides were performed using Lipofectamine 2000 (Invitrogen).

Cell proliferation and colony formation assays. Cells were seeded into 96-well plates at 1×10^3 cells/well and counted in triplicate on day 4 or 5 by using Cell Counting kit 8 (CK04-11; Dojindo, Rockville, MD). For colony formation assays, cells were seeded into 12-well plates at 2×10^2 to 3×10^2 cells/well. Medium was changed every other day. Two weeks later, colonies were fixed in 4% paraformaldehyde for 15 min and stained with 0.5% crystal violet–20% methanol in PBS for 30 min. Images were captured using the Chemidoc system (Bio-Rad, Hercules, CA), and colonies were counted using QuantityOne software (Bio-Rad).

Immunoblotting and immunostaining. For immunoblotting, cells were lysed in NETN buffer (10 mM Tris [pH 8.0], 1% NP-40, 150 mM NaCl, 1 mM EDTA, and protease inhibitor cocktail). To detect the level of p-H3 (Ser10), lysates were vortex mixed three times for 30 s each. Samples were resolved by SDS-PAGE, transferred to nitrocellulose membranes, and incubated with antibodies. Bound antibodies were detected using a chemiluminescence detection kit (Pierce).

For immunostaining, cells cultured on coverslips were washed with PBS and fixed in either 4% paraformaldehyde for 15 min at room temperature or ice-cold methanol for 20 min at −20°C. Fixed cells were permeabilized in PBS containing 0.5% Triton X-100 for 5 min and blocked in 3% bovine serum albumin in PBS for 30 min. Cells were then incubated with primary antibodies at 4°C overnight, followed by a 1-h incubation with secondary antibody. Cells were washed, and nuclei were counterstained with 4′,6-diamidino-2-phenylindole (DAPI; Invitrogen) and mounted with Vectashield mounting medium (Vector Laboratories, Burlingame, CA). Images were captured using an automated upright/inverted fluorescence microscope (Zeiss, Peabody, MA). The mitotic index was determined by counting at least 500 cells in 5 or 6 fields.

Flow cytometric analysis. To determine the cell cycle DNA distribution, H1299 cells expressing control shGFP or shRNA targeting *HDAC10* were harvested by trypsinization at various time points after synchronization and fixed with 70% ethanol. Approximately 10^6 cells were incubated with a propidium iodide (PI) mixture (50 μg/ml PI, 100 μg/ml RNase A, 0.1% Triton X-100 in PBS); DNA content was determined using a FACSCalibur flow cytometer and analyzed using CellQuest software (Becton Dickinson, Sparks, MD). To determine the mitotic index based on immunostaining of p-H3 (Ser10), cells were permeabilized in 0.25% Triton X-100 in PBS on ice for 5 min and incubated with anti-p-H3 (Ser10) antibody (1:400), followed by Alexa Fluor 488-conjugated goat anti-rabbit antibody (1:200), both in PBS containing 1% bovine serum albumin. Cells underwent final staining with PI.

An EdU incorporation assay was performed using the Click-iT EdU Alexa Fluor 488 flow cytometry assay kit (Invitrogen) according to the manufacturer's instructions. Briefly, cells were pulse-labeled with 10 μM EdU for 1, 2, 4, 6, and 8 h at 37°C, harvested, and fixed in 70% ethanol. Cells were stained with anti-p-H3 (Ser10) antibody and Alexa Fluor 568-conjugated goat anti-rabbit IgG, followed by Alexa Fluor 488 EdU detection reagent. DNA was stained with 1 μg/ml DAPI and measured using a FACSCalibur apparatus.

Luciferase reporter assay. *HDAC10* knockdown and control H1299 cells grown in 24-well plates were transfected with 100 ng cyclin A2 promoter luciferase reporter plasmid together with 2 ng *Renilla* luciferase construct (pRL-TK). To assess the effect of HDAC10 overexpression on cyclin A2 promoter activity, HEK 293T cells in 24-well plates were cotransfected with 400 ng expression vector encoding FLAG-tagged HDAC10 or control vector and 100 ng promoter reporter plasmids. Transfection mixtures were spiked with pRL-TK for normalization of firefly luciferase activity. Luciferase activity was detected using the Dual-Luciferase reporter assay system (Promega) following the manufacturer's protocol.

The HMGA2-3′ UTR reporter assay was performed as described previously (37). Briefly, *HDAC10* knockdown and control H1299 cells were transfected with HMGA2-3′ UTR or mutant HMGA2-3′ UTR-m7 *Renilla* luciferase reporters together with firefly luciferase reporter plasmid pGL3-control as internal control. In HEK 293T cells, the HMGA2-3′ UTR or HMGA2-3′ UTR-m7 reporter was cotransfected with the FLAG-tagged HDAC10 vector or control vector. Firefly and *Renilla* luciferase activities were measured 48 h after transfection using the Dual-Luciferase reporter assay system.

ChIP assay. A chromatin immunoprecipitation (ChIP) assay was performed essentially as described previously (38). Cells were incubated for 10 min in 1% formaldehyde, followed by addition of 0.125 M glycine and sonication to generate DNA fragments of 200 to 1,000 bp. Chromatin from $\sim 1.5 \times 10^6$ cells was incubated overnight at 4°C with 2 to 5 μg anti-FLAG, anti-HDAC10, anti-V5, anti-histone H3, anti-acetyl-histone H3 (Lys9), anti-acetyl-histone H3 (Lys14), anti-acetyl-histone H3 (Lys18), anti-acetyl-histone H3 (Lys27), and anti-acetyl-histone H4 (Lys5) antibodies. Normal mouse and rabbit IgG (Upstate Biotechnology, Lake Placid, NY) were used as controls. Samples were incubated with preblocked protein A/G Plus beads (catalog number 2003; Santa Cruz Biotechnology) for 2 h at 4°C. DNA was purified and amplified by PCR using the primers shown in Table S1 in the supplemental material. Primers for LET7F2/98-8 (VDRE-A), LET7F2/98-9 (VDRE-B), LET7F2/98-10 (VDRE-C), LET7C/99A-TSS-COR, LET7C/99A-RARE-OZ, and LET7C/99A-TSS-OZ were described previously (39, 40).

qPCR. Total RNA was isolated from cells with TRIzol reagent (Invitrogen). Reverse transcription was carried out using the qScript cDNA synthesis kit (Quanta Biosciences, Gaithersburg, MD). Relative quantitation of mRNAs was carried out via SYBR green-based quantitative PCR (qPCR). iQ SYBR green Supermix (Bio-Rad) according to the manufacturer's instructions, and PCR was carried out using a 7900HT Fast real-time PCR system (Applied Biosystems) under the following conditions: 95°C for 10 min, followed by 40 cycles of 95°C for 15 s and 60°C for 60 s. 18S rRNA served as an internal control. PCR results were analyzed using the $2^{-(\Delta\Delta CT)}$ method. TaqMan miRNA assays for miR-98 (000577) and *let-7f* (000382; Applied Biosystems) were used to determine levels of the mature miRNAs. U6 snRNA (001973) served as an internal control.

To assess gene expression as a function of cell cycle, total RNA was isolated from *HDAC10* knockdown and control H322 cells by using the mirVana miRNA isolation kit (Applied Biosystems) and reverse transcribed into cDNA using the RT^2 first strand kit (Qiagen, Valencia, CA); the cDNA was amplified using the RT^2 Profiler PCR arrays human cell cycle sytem (Qiagen) according to the manufacturer's instructions. Data

FIG 2 HDAC10 is required for mitotic entry. (A) Flow cytometric analysis of cell cycle distribution of propidium iodide-stained *HDAC10* knockdown and control H1299 (left) and H322 (right) cells. (B) Flow cytometric analysis of cell cycle distribution of synchronized H1299 cells expressing the indicated control shRNA or shRNA targeting HDAC10 released at the indicated times from double-thymidine block. (Left) DNA content distribution analyzed by PI staining; (right) percentages of M or G_2/M cells, calculated by dividing the proportion of p-H3 (Ser10)-positive cells (mitotic index) by that of G_2/M cells at each time point. (C) Results of flow cytometric analysis of EdU incorporation by S-phase cells (left), the proportion of phospho-histone H3 (Ser10)-positive mitotic cells in the EdU^+ population at the indicated times (middle), and the DNA content (*x* axis) together with EdU intensity (*y* axis) at 8 h after EdU incorporation (right). (D, left) Immunostaining of p-H3 (Ser10) in H1299 cells expressing the indicated shRNAs and synchronized at M phase by nocodozole treatment; nuclei were counterstained with DAPI. (Right) Western blot analysis results for HDAC10 and p-H3 (Ser10) in the cells shown at left. (E) Immunostaining of tubulin (red) in HeLa cells expressing the indicated shRNAs (left) and mitotic indices (right) at the indicated times after release from RO-3306 block in G_2. Cells were counterstained with DAPI (blue). (F) Fluorescence analysis of tubulin (red) and DAPI (blue) in *HDAC10* knockdown and control HeLa cells after treatment with RO-3306 to block cells at the G_2 phase. (G) Mitotic indices of cells expressing the indicated shRNAs and transfected with an expression vector encoding shRNA-resistant *HDAC10* or control vector, 40 min after release from RO-3306. Values represent means ± standard deviations. *, $P < 0.05$.

were analyzed using the $2^{-(\Delta\Delta CT)}$ method with normalization to housekeeping genes.

Tumor growth in SCID mice. Six-week-old female severe combined immune deficiency beige (SCID-Bg) mice (Taconic Biosciences, Germantown, NY) were maintained under appropriate conditions. A549-luc cells were transduced with lentiviral *HDAC10*-specific shRNA (A549-luc-shHDAC10) or control green fluorescent protein (GFP) shRNA (A549-luc-shGFP) and selected in 1.5 μg/ml puromycin for 5 days. A549-luc-sh*HDAC10* and A549-luc-shGFP cells (2.4×10^6) were injected subcutaneously in the right and left flanks, respectively, of SCID mice. Mice were evaluated weekly for tumor development by bioluminescence imaging using an IVIS 200 imaging system (Xenogen, Alameda, CA). Seven weeks after implantation, mice were sacrificed, and tumor weights and diameters were measured. Tumor volume was calculated using the following formula: volume (in cubic millimeters) = $(\text{width})^2 \times \text{length}/2$.

RNA sequencing and data analysis. Total RNA was isolated from *HDAC10* knockdown and control H1299 cells, and HDAC10 wild-type and knockout MEFs by using the mirVana miRNA isolation kit (Applied Biosystems). RNA sequencing libraries were constructed from 1 μg RNA, and sequencing was carried out using Illumina Hiscan SQ sequencers, which generated 100-bp paired-end reads for each library. Reads were aligned using TopHat, and the output file was converted to BED format with the bamToBed script from the BEDTools package (http://bedtools.readthedocs.org/en/latest/). The BEDTools coverageBed script was used to derive read counts for individual exons in the RefSeq database (http://www.ncbi.nlm.nih.gov/refseq/). A total count for each transcript in this database was obtained by adding the counts for its constituent exons.

Statistical analysis. Statistical analyses were carried out using SPSS 11.0 software (IBM, Armonk, NY). Statistical significance was determined using Student's *t* test, with a *P* level of <0.05 considered statistically significant. Data are representative of at least three independent experiments conducted in triplicate.

RESULTS

HDAC10 regulates tumor cell proliferation *in vitro* and *in vivo*. To study the effect of HDAC10 on cell proliferation, the lentiviral system was used to transduce *HDAC10*-specific shRNA into H1299 and H322 cells, in which HDAC10 is highly expressed. Knockdown efficiency was confirmed by qPCR (data not shown) and Western blotting (Fig. 1A). Three shRNAs, targeting different regions of *HDAC10* mRNA, effectively repressed expression of endogenous *HDAC10*. Colony formation indicated that *HDAC10* knockdown significantly suppressed cell proliferation (Fig. 1A). To validate that this effect was HDAC10 specific, we constructed an expression plasmid harboring shRNA-resistant *HDAC10* and performed a rescue experiment. Overexpression of shRNA-resistant *HDAC10* abolished shRNA-induced cell growth arrest (Fig. 1B). Furthermore, *HDAC10* knockout MEFs had decreased cell viability compared to wt MEFs (Fig. 1C), and overexpression of ectopic *HDAC10* in *HDAC10* knockout MEFs promoted cell proliferation (Fig. 1D).

To determine if HDAC10 is required for cell growth *in vivo*, a mouse xenograft model was used to examine the effect of *HDAC10* knockdown on tumor growth. HDAC10 knockdown and control luciferase-expressing A549 cells were subcutaneously implanted into the right and left flanks of SCID-bg mice ($n = 5$), respectively. Tumor growth was monitored weekly by *in vivo* imaging. Bioluminescence quantitation showed that, 3 weeks after inoculation, growth of tumors from HDAC10 knockdown cells was significantly inhibited (Fig. 1E and F). Seven weeks after implantation, the mice were sacrificed; the mean tumor weights and volumes for mice implanted with *HDAC10* knockdown cells were lower than in mice implanted with control cells (Fig. 1G). These results indicated that HDAC10 is also crucial for tumor growth *in vivo*.

***HDAC10* knockdown inhibits mitotic entry.** To explore how HDAC10 affected cell proliferation, cell cycle analysis by flow cytometry was carried out. In both H1299 and H322 cells, *HDAC10* knockdown with each of three shRNAs induced cell cycle arrest at G_2/M (Fig. 2A).

To determine more precisely which phase of the cell cycle was affected by *HDAC10* knockdown, cells were synchronized and arrested in S phase by a double-thymidine block. Significant accumulation of knockdown cells in G_2/M was seen 8 to 12 h after release from block (Fig. 2B, left). Lack of an increase in the percentage of mitotic cells, relative to controls (Fig. 2B, right), suggested that the *HDAC10* knockdown cells were delayed at the G_2/M boundary. Despite a larger overall G_2/M population, the *HDAC10* knockdown cells were unable to proceed from G_2 into mitosis.

Analysis of the time course for the S-to-M transition was performed using EdU incorporation followed by detection of phosphorylated histone H3 (Ser10; p-H3 [Ser10]). Cells were labeled with EdU, and EdU^+ mitotic cells were counted by flow cytometry. Control and *HDAC10* knockdown cells had similar EdU incorporation rates, which indicated that knockdown did not affect S-phase DNA synthesis (Fig. 2C, left). However, the number of EdU^+ mitotic knockdown cells was significantly lower than the number of control cells, although the total number of EdU^+ G_2/M cells was increased in the knockdown cells (Fig. 2C, middle and right). By either EdU incorporation assay or double-thymidine block, the lack of increase in the mitotic index of the HDAC10 knockdown cells reflected arrest at the G_2/M boundary, which indicated that *HDAC10* knockdown delays mitotic entry.

To confirm this result, cells were treated with nocodazole to synchronize mitotic cells. Immunofluorescence and Western analyses showed that nocodazole treatment resulted in a significant decrease of p-H3 (Ser10) in *HDAC10* knockdown cells compared to control cells (Fig. 2D). Because p-H3 (Ser10) is a marker of mitosis and *HDAC10* knockdown inhibited entry into mitosis upon nocodazole treatment, loss of p-H3 (Ser10) in knockdown cells indicated arrest at the G_2 checkpoint.

In addition to the use of p-H3 (Ser10) as a marker, mitotic morphology was assessed by α-tubulin staining. HeLa cells were blocked at the G_2/M transition by treatment with RO-3306, a specific inhibitor of CDK1. Release from the block allowed control cells to rapidly enter into mitosis, which peaked after 30 to 40 min, but the knockdown cells remained in prophase (Fig. 2E). Proper centrosome separation and bipolar spindle assembly were not observed in RO-3306-treated knockdown cells (Fig. 2F), which indicated that *HDAC10* knockdown-induced cell cycle arrest occurred before CDK1 activation. HDAC10 overexpression rescued the cells from knockdown-mediated mitotic arrest (Fig. 2G), which demonstrated the specific effect of HDAC10 loss on G_2 arrest.

HDAC10-regulated cyclin A2 expression. To explore which cell cycle-related genes were involved in HDAC10-mediated G_2/M phase regulation, a cell cycle PCR array was used to compare gene expression profiles of *HDAC10* knockdown and control cells. *CCNA2*, which encodes cyclin A2, showed a 2-fold decrease in expression in knockdown cells (Fig. 3A). Cyclin A2, the major A-type cyclin in mammals, is required for completion of prophase. Previous reports suggested that loss of cyclin A2 induced cell cycle arrest at G_2 and resulted in a substantial delay in chro-

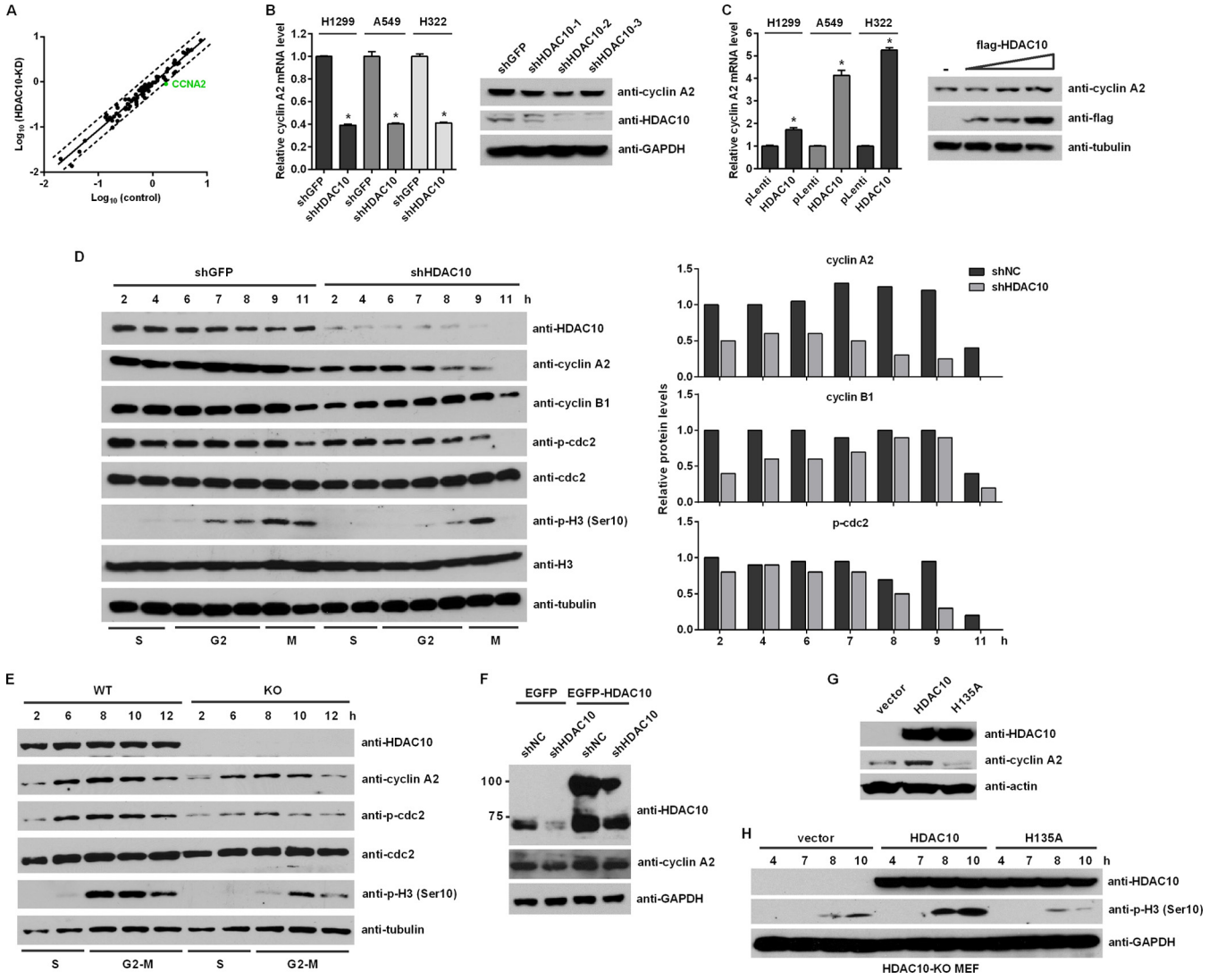

FIG 3 HDAC10 regulates cyclin A2 expression. (A) Results of PCR array analysis of expression of cell cycle-related genes in *HDAC10* knockdown cells compared with control H322 cells. Cyclin A2 (CCNA2) is shown in green. Dashed lines indicate a 2-fold change in the gene expression threshold. (B and C, left) PCR analysis of cyclin A2 mRNA levels in the indicated cell types expressing control shRNA (shGFP), shRNA targeting HDAC10 (shHDAC10), or control vector (pLenti) or HDAC10 expresssion vector (HDAC10). (Right) Western blot analysis of cyclin A2 and HDAC10 levels. GAPDH and tubulin served as internal controls. Values are means ± standard deviations. *, $P < 0.05$. (D, left) Western analysis of the indicated proteins in *HDAC10* knockdown and control H1299 cells synchronized in S phase and released from hydroxyurea block at the indicated times. (Right) Quantified protein levels of cyclin A2, B1, and p-cdc2 in Western blot analysis. (E) Western blot analysis of HDAC10 wild-type (WT) and knockout (KO) MEFs at the indicated times after release from hydroxyurea block in S phase. (F) Western blot analysis of *HDAC10* knockdown and control H1299 cells 72 h after transient transfection with GFP-tagged shRNA-resistant *HDAC10* expression plasmid or control vector. (G) Western analysis of cyclin A2 in *HDAC10* knockout MEFs transduced with control lentiviral vector or lentiviral vectors encoding wild-type or H135A mutant HDAC10. (H) Western blot analysis of p-H3 (Ser10) during the S-to-M transition in *HDAC10* knockout MEFs transduced with lentiviral vector alone or vector encoding wild-type or H135A mutant HDAC10 synchronized in S phase and released from hydroxyurea block at the indicated times.

matin condensation and H3 (Ser10) phosphorylation (41–43). Therefore, we hypothesized that *HDAC10* knockdown-induced accumulation in G_2 was due to loss of cyclin A2 expression. qPCR and Western analysis of H1299, A549, and H322 cells showed that HDAC10 knockdown decreased levels of cyclin A2 mRNA and protein, whereas HDAC10 overexpression increased the cyclin A2 level (Fig. 3B and C).

To detect the dynamic changes in cyclin A2 during the S-M phase transition, cells were synchronized in S phase by serum starvation followed by hydroxyurea treatment. Phosphorylation of H3 (Ser10) in *HDAC10* knockdown cells was reduced during the G_2/M transition, indicating arrest at mitotic entry (Fig. 3D). Analysis showed that cyclin A2 was significantly downregulated in *HDAC10* knockdown cells, along with modest reductions in cyclin B and phospho-cdc2 (Fig. 3D, right). Similar results were obtained in *HDAC10* knockout MEFs (Fig. 3E). Overexpression of shRNA-resistant *HDAC10* rescued cyclin A2 expression in H1299 knockdown cells and in *HDAC10* knockout MEFs, which demonstrated the specific effect of HDAC10 loss on cyclin A2 expression (Fig. 3F and G). How-

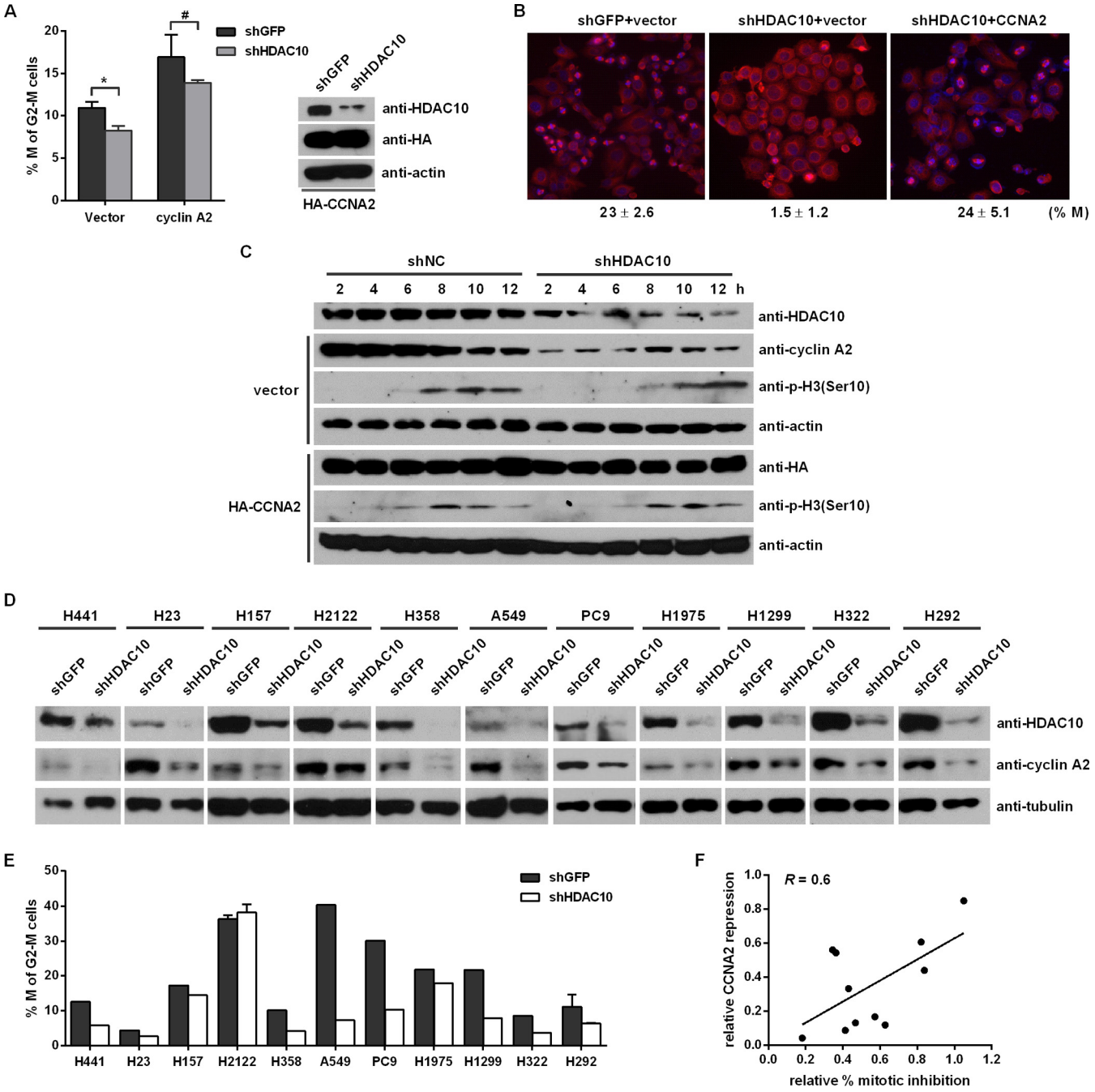

FIG 4 The effect of HDAC10 on the G_2/M transition is dependent on cyclin A2. (A) Mitotic indices (left) and Western analysis results (right) for H1299 cells expressing control shRNA (shGFP) or shRNA targeting HDAC10 and transfected with control or cyclin A2 expression plasmid. *, $P < 0.05$; #, $P > 0.05$. (B) Fluorescence analysis of tubulin (red) and DAPI (blue) in control (left) and *HDAC10* knockdown (middle and right) HeLa cells transfected with control (left and middle) or cyclin A2 expression plasmid (right) after release from RO-3306 block in G_2. (C) Western analysis of p-H3 (Ser10) during the S-to-M transition in *HDAC10* knockdown and control H1299 cells transfected with vector alone or vector encoding hemagglutinin (HA)-tagged CCNA2 synchronized in S phase and released from double-thymidine block at the indicated times. (D and E) Western blot analysis results for HDAC10 and cyclin A2 (D) and the mitotic indices of human NSCLC cell lines transduced with control lentiviral vector or lentiviral vector harboring HDAC10-shRNA lentivirus (E). (F) Dot plot demonstrating the correlation between cyclin A2 repression and the extent of mitotic arrest in *HDAC10* knockdown cells.

ever, the catalytically inactive HDAC10 H135A mutant did not enhance cyclin A2 expression or promote entry into mitosis (Fig. 3G and H), which indicated that the effect of HDAC10 on cyclin A2 expression was dependent on HDAC10 deacetylase activity.

***HDAC10* knockdown decreased cyclin A2 levels and contributed to G_2/M arrest.** To address whether HDAC10 regulates the G_2/M transition via cyclin A2, a rescue assay was performed to confirm that delayed mitotic entry of *HDAC10* knockdown cells was due to cyclin A2 downregulation. Cell cycle distribution anal-

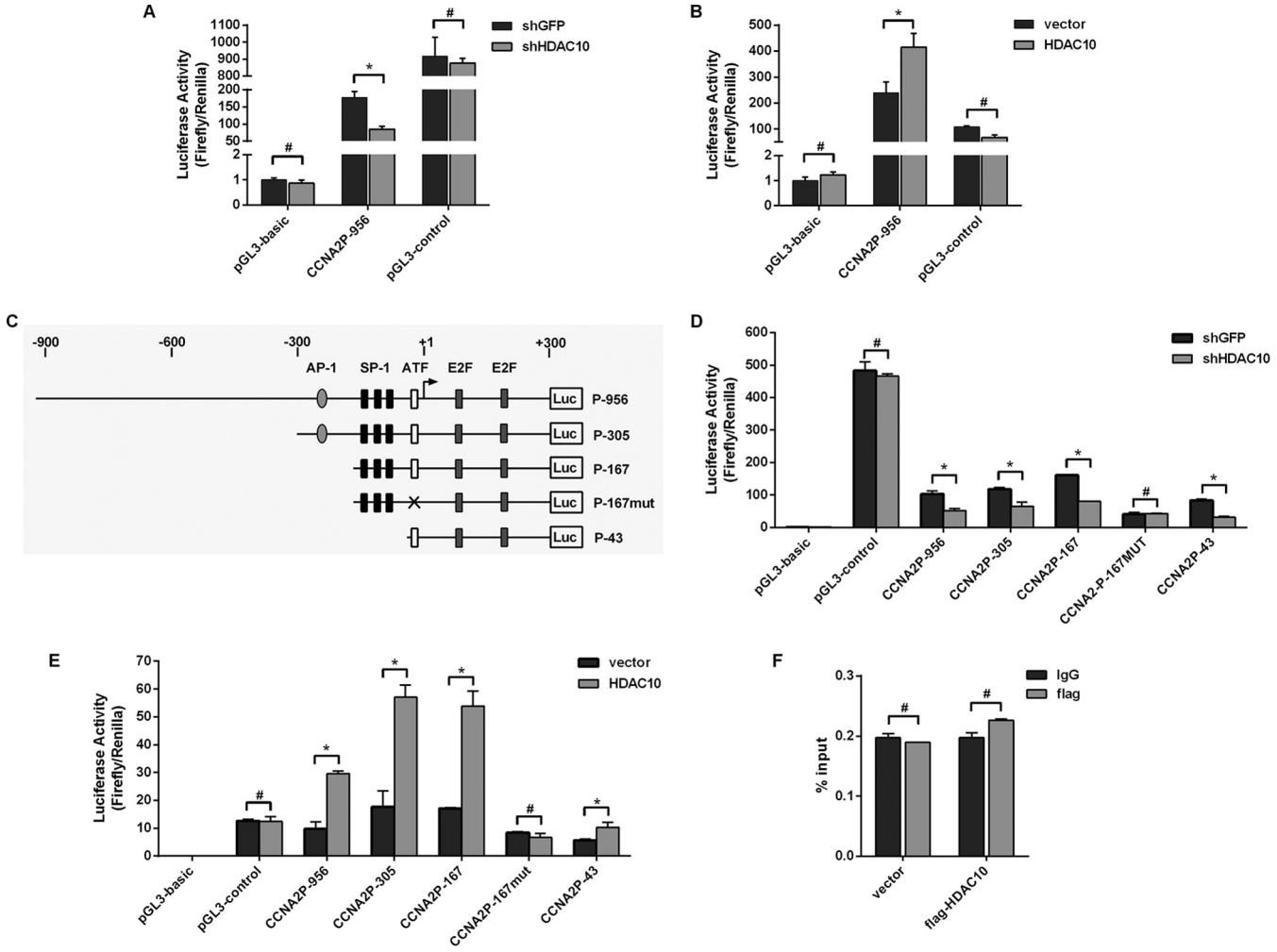

FIG 5 HDAC10 regulates cyclin A2 promoter activity through ATF/CRE-binding sites. (A) Results of the reporter assay of *HDAC10* knockdown (shHDAC10) and control (shGFP) H1299 cells transfected with the indicated pGL3 luciferase reporter vectors or pRL-TK *Renilla* expression vector. (B) Results of the reporter assay with HEK 293T cells transfected with FLAG-tagged HDAC10 expression vector or control vector, the indicated pGL3 luciferase reporter vectors, and pRL-TK *Renilla* luciferase expression vector. (C) Schematic representation of the luciferase reporter vectors used. The region of the human cyclin A2 (CCNA2) promoter between bp −956 and +306 was cloned into the pGL3-Basic vector to generate plasmid CCNA2P-956. The other plasmids were obtained by serial deletion of CCNA2P-956. The ATF/CRE site in reporter plasmid CCNA2P-167 was mutated to generate plasmid CCNA2P-167mut. (D) Results of the reporter assay with *HDAC10* knockdown and control H1299 cells transfected with the indicated reporter vectors and *Renilla* expression vector. (E) Results of the reporter assay of HEK 293T cells transfected with FLAG-tagged HDAC10 expression vector or control vector together with the indicated reporter vectors and pRL-TK *Renilla* expression vector. (F) HEK 293T cells were transfected with FLAG-tagged HDAC10 or control vector. Results of the ChIP analysis of the human cyclin A2 promoter region using anti-FLAG antibody are shown. Normal IgG was used as the control antibody. qPCR data are expressed as the percentage relative to their respective input. Values are means ± standard deviations. *, $P < 0.05$; #, $P > 0.05$.

ysis showed that cyclin A2 overexpression abolished *HDAC10* knockdown-induced mitotic arrest (Fig. 4A). Ectopic cyclin A2 expression significantly increased the mitotic index of *HDAC10* knockdown cells after release from RO-3306 block-induced G_2/M arrest (Fig. 4B). To further detect the role of cyclin A2 in *HDAC10* knockdown-induced mitotic entry arrest, HDAC10 knockdown and control H1299 cells were synchronized in S phase by a double-thymidine block and release at various time points. Phosphorylation of H3 (Ser10) in *HDAC10* knockdown cells was delayed (2 to 4 h) during the G_2/M transition, and cyclin A2 overexpression could override the delay of appearance of phospho-histone H3 in *HDAC10* knockdown cells (Fig. 4C). These results indicated HDAC10 regulates G_2/M transition through cyclin A2.

To examine whether *HDAC10* knockdown-induced cell cycle arrest is universal, *HDAC10* was knocked down in a panel of NSCLC cell lines. In nearly all cell lines tested, the cyclin A2 level was significantly decreased with *HDAC10* knockdown (Fig. 4D). Flow cytometric analysis showed that the mitotic indices of most NSCLC knockdown cells were lower than those of control cells (Fig. 4E). Additionally, the extent of mitotic inhibition correlated positively with that of cyclin A2 reduction in *HDAC10* knockdown cells (Fig. 4F).

HDAC10 regulates cyclin A2 promoter activity via ATF/CRE binding sites. To investigate the mechanism underlying decreased cyclin A2 mRNA expression in *HDAC10* knockdown cells, we examined the effect of HDAC10 on cyclin A2 promoter activity. The entire cyclin A2 promoter (nucleotides −956 to +306) was inserted into the luciferase reporter vector

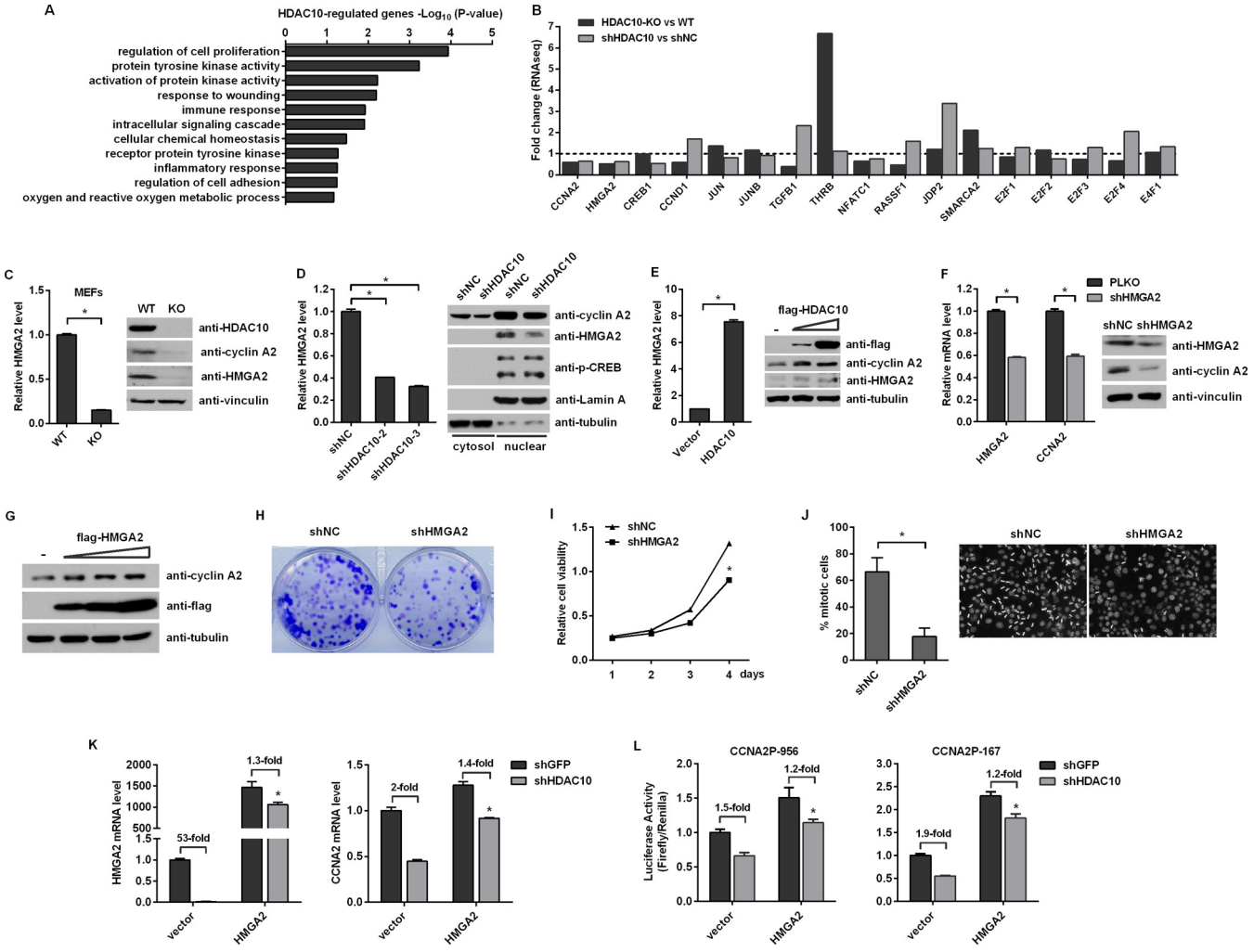

FIG 6 HDAC10 regulates HMGA2 expression. (A) Results of gene ontology analysis, performed using DAVID tools (http://david.abcc.ncifcrf.gov/), of differentially expressed genes identified by comparative RNA sequencing of *HDAC10* knockdown and control H1299 cells. (B) Results of comparative RNA sequence analysis of gene expression profiles of *HDAC10* knockdown H1299 cells (shHDAC10) and knockout MEFs (HDAC10-KO). The relative expression levels of genes related to regulation of cyclin A2 transcription were normalized to the respective control group (shNC and WT), and the latter was set to 1. (C and D) qPCR (left) and Western blot analyses (right) of HMGA2 mRNA and protein levels, respectively, in wild-type (WT) and *HDAC10* (KO) MEFs (C) and control (shNC) and *HDAC10* knockdown (shHDAC10-2 and -3) H1299 cells (D). (E) qPCR (left) and Western blot analysis (right) of HMGA2 in HEK 293T cells transfected with vector alone or FLAG-HDAC10. (F) qPCR analysis (left) and Western analysis (right) of HMGA2 and cyclin A2 (CCNA2) in H1299 cells transduced with control (shNC) or HMGA2 shRNA lentiviral vector. Vinculin served as the internal control. (G) Western analysis of HEK 293T cells transfected with vector control or increasing amounts of FLAG-HMGA2 expression vector, 72 h posttransfection. (H and I) Colony formation assay (H) and relative viability (I) of H1299 cells transduced with control (shNC) or HMGA2 shRNA lentiviral vector. (J) Mitotic indices (left) and micrographs (right) of HMGA2 knockdown cells after release from RO-3306 arrest. (K) qPCR analysis of *HMGA2* and cyclin A2 mRNA levels in *HDAC10* knockdown and control H1299 cells 48 h posttransfection with control (vector) or an HMGA2 expression plasmid. (L) Reporter assay results with *HDAC10* knockdown and control H1299 cells transfected with control or HMGA2 expression plasmid and the indicated cyclin 2A (*CCNA2*) promoter reporter plasmid. *, $P < 0.05$.

pGL3-Basic. *HDAC10* knockdown decreased, and HDAC10 overexpression promoted, luciferase activity (Fig. 5A and B), which suggested that HDAC10 regulates transcription from the cyclin A2 promoter.

Reporter plasmids that contained a truncated promoter sequence generated by serial deletion of the full-length reporter plasmid (Fig. 5C) were expressed in *HDAC10* knockdown (Fig. 5D) and HDAC10-overexpressing (Fig. 5E) cells. Results indicated that HDAC10 regulates cyclin A2 promoter activity via the ATF/CRE binding site. However, ChIP showed no direct binding between HDAC10 and the promoter (Fig. 5F), which indicated that the effect of HDAC10 on cyclin A2 promoter activity likely does not result from HDAC10's histone deacetylase activity surrounding the promoter.

Transcriptional repression of cyclin A2 in *HDAC10* knockdown cells is associated with loss of HMGA2. To determine what factor(s) might mediate HDAC10 regulation of cyclin A2, comparative RNA sequencing was used to analyze gene expression profiles of *HDAC10* knockdown H1299 cells and knockout MEFs. Gene ontology analysis demonstrated that genes related to cell proliferation regulation showed the most statistically significant changes in *HDAC10* knockdown cells (Fig. 6A). Among the genes previously reported to be involved in cyclin A2 promoter regulation, HMGA2 (high-mobility group AT-hook 2) expression was

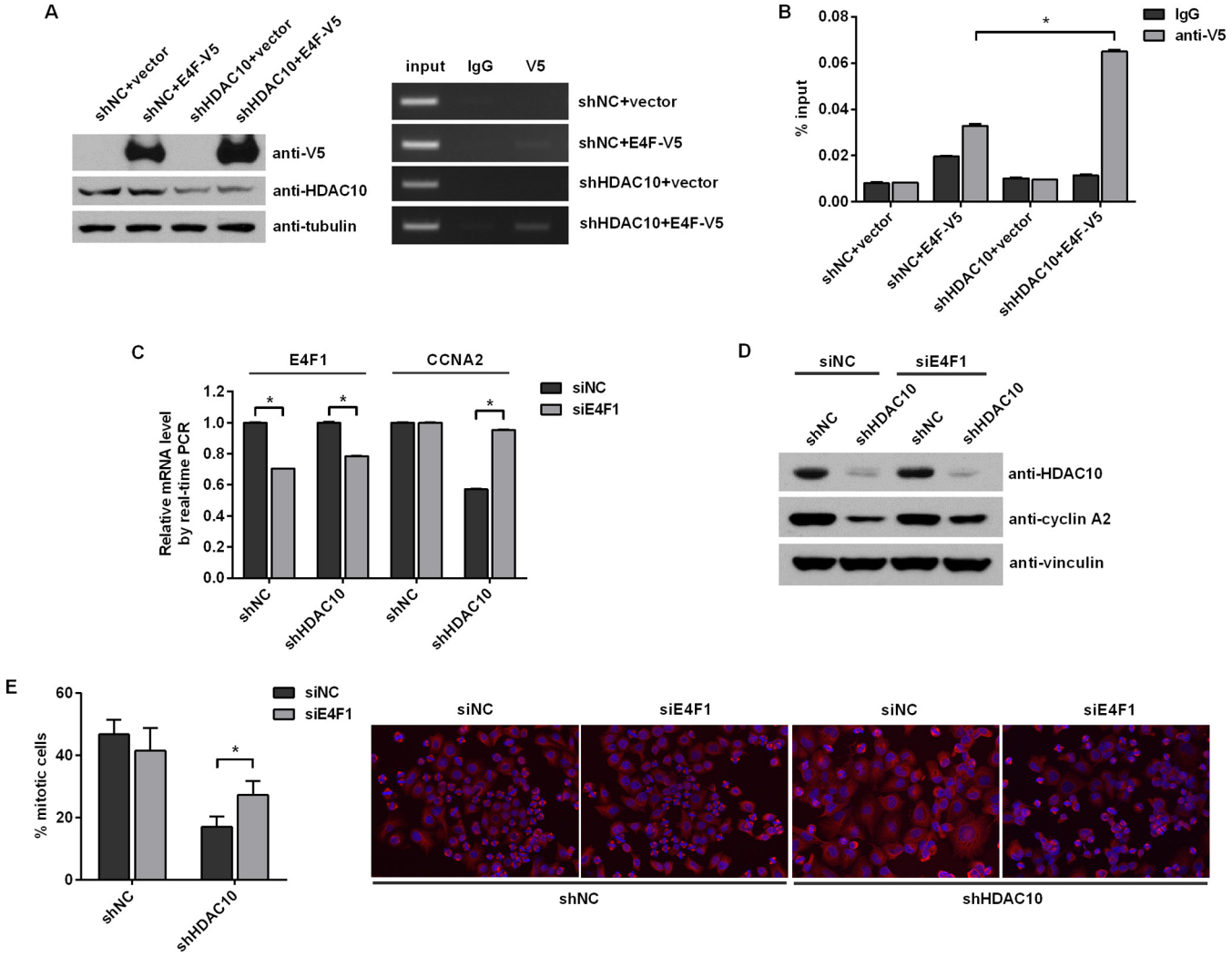

FIG 7 E4F1-dependent regulation of cyclin A in *HDAC10* knockdown cells. (A) Western blot analysis of control (shNC) and *HDAC10* knockdown (shHDAC10) H1299 cells transfected with vector alone or V5-tagged E4F (left) and separated, PCR-amplified fragments of the human cyclin A2 promoter in a 2% agarose gel (right) after ChIP with anti-V5 or control IgG were analyzed. (B) qPCR amplification of ChIP results, expressed as the percentage of respective input. (C and D) qPCR (C) and Western analysis (D) of E4F1 and cyclin A2 levels in *HDAC10* knockdown and control H1299 cells 48 h posttransfection with control (siNC) or E4F1-specific siRNA (siE4F1). (E) Mitotic indices (left) and micrographs (right) of cells expressing the indicated shRNAs and transfected with siNC or siE4F1, 40 min after release from RO-3306. Values are means ± standard deviations. *, $P < 0.05$.

reduced in both knockdown and knockout cells (Fig. 6B), as confirmed by qPCR and Western analysis (Fig. 6C and D). HDAC10 overexpression increased the HMGA2 level (Fig. 6E).

HMGA2 was directly associated with the transcriptional repressor $p120^{E4F}$ (E4F1), which interfered with $p120^{E4F}$ binding to the ATF/CRE site on the cyclin A2 promoter, and activated the promoter (34); thus, HMGA2 positively regulated cyclin A2 expression. Cyclin A2 mRNA and protein levels were reduced by *HMGA2* knockdown and increased by HMGA2 overexpression (Fig. 6F and G). If HMGA2 is the key factor mediating cyclin A2 regulation in *HDAC10* knockdown cells, *HMGA2* knockdown cells should have a similar phenotype as the *HDAC10* knockdown cells. *HMGA2* knockdown suppressed cell proliferation (Fig. 6H and I) and inhibited mitotic entry after release from RO-3306 block in G_2 (Fig. 6J). HMGA2 overexpression partially abrogated *HDAC10* knockdown-induced transcriptional repression of cyclin A2 mRNA expression (Fig. 6K) and promoter activities (Fig. 6L), which confirmed that HMGA2 played an important role in HDAC10-mediated cyclin A2 transcription regulation. However, we cannot exclude that other factors might be involved in HDAC10-related cyclin A2 regulation.

HMGA2 interacted with $p120^{E4F}$ and activated the cyclin A2 promoter by counteracting the repressive activity of $p120^{E4F}$ via the ATF/CRE site (34). Consistent with the finding that HMGA2 was downregulated in *HDAC10* knockdown cells, the ChIP assay of *HDAC10* knockdown H1299 cells demonstrated 2-fold enrichment of $p120^{E4F}$ at the cyclin A2 promoter region compared with control cells (Fig. 7A and B). Depletion of $p120^{E4F}$ in *HDAC10* knockdown cells could also partially rescue the transcriptional repression of cyclin A2 (Fig. 7C and D) as well as G_2/M arrest (Fig. 7E), supporting HMGA2's involvement in the *HDAC10* knockdown-mediated cyclin A2 regulation.

HDAC10 regulates HMGA2 by direct suppression of *let-7f-2*/miR-98 transcription. Several pieces of evidence indicated that

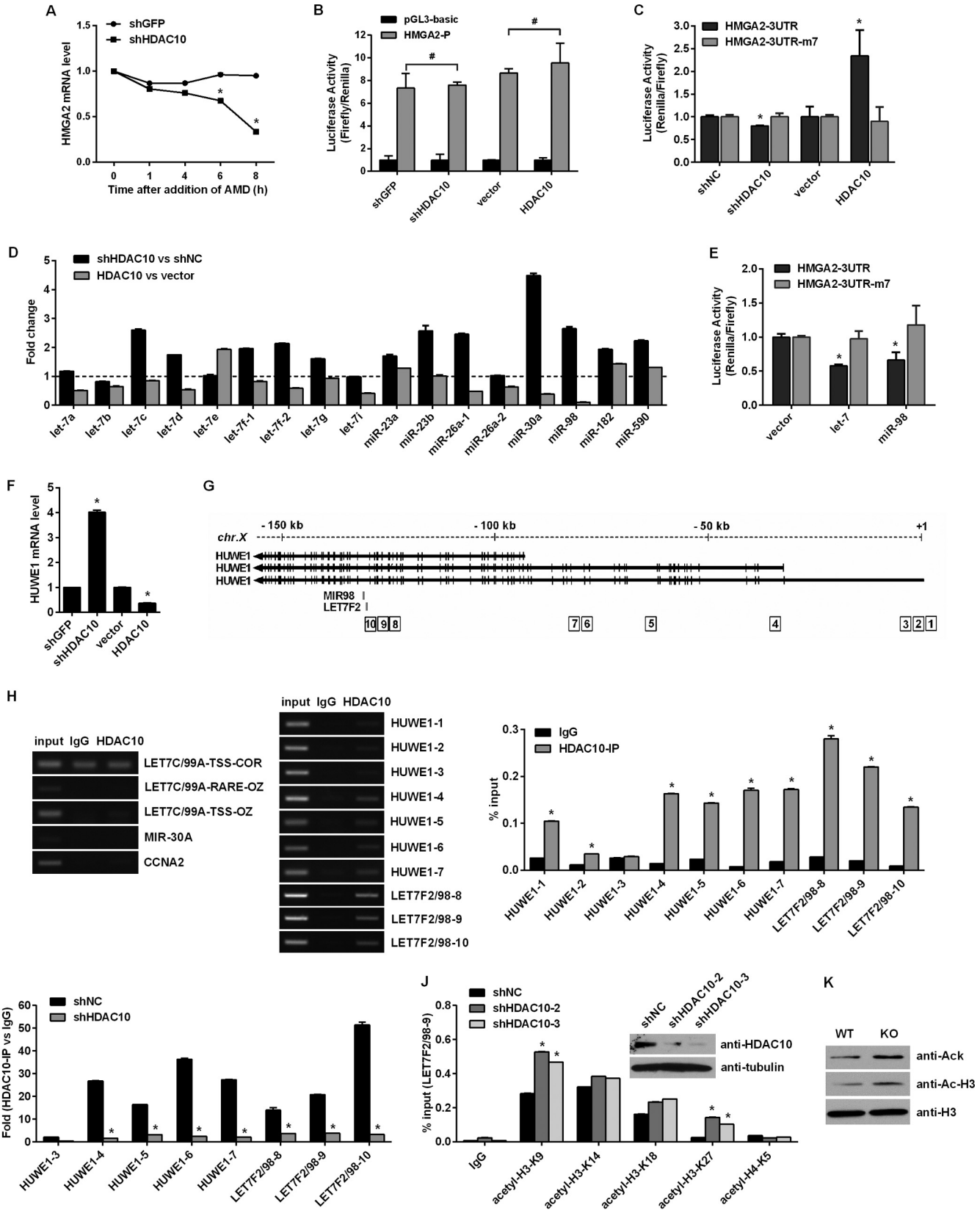
A
shGFP
shHDAC10
HMGA2 mRNA level
Time after addition of AMD (h)
B
pGL3-basic
HMGA2-P
Luciferase Activity (Firefly/Renilla)
shGFP
shHDAC10
vector
HDAC10
C
HMGA2-3UTR
HMGA2-3UTR-m7
Luciferase Activity (Renilla/Firefly)
shNC
shHDAC10
vector
HDAC10
D
shHDAC10 vs shNC
HDAC10 vs vector
Fold change
let-7a
let-7b
let-7c
let-7d
let-7e
let-7f-1
let-7f-2
let-7g
let-7i
miR-23a
miR-23b
miR-26a-1
miR-26a-2
miR-30a
miR-98
miR-182
miR-590
E
HMGA2-3UTR
HMGA2-3UTR-m7
Luciferase Activity (Renilla/Firefly)
vector
let-7
miR-98
F
HUWE1 mRNA level
shGFP
shHDAC10
vector
HDAC10
G
chr.X
-150 kb
-100 kb
-50 kb
+1
HUWE1
HUWE1
HUWE1
MIR98
LET7F2
H
input IgG HDAC10
LET7C/99A-TSS-COR
LET7C/99A-RARE-OZ
LET7C/99A-TSS-OZ
MIR-30A
CCNA2
input IgG HDAC10
HUWE1-1
HUWE1-2
HUWE1-3
HUWE1-4
HUWE1-5
HUWE1-6
HUWE1-7
LET7F2/98-8
LET7F2/98-9
LET7F2/98-10
IgG
HDAC10-IP
% input
I
shNC
shHDAC10
Fold (HDAC10-IP vs IgG)
HUWE1-3
HUWE1-4
HUWE1-5
HUWE1-6
HUWE1-7
LET7F2/98-8
LET7F2/98-9
LET7F2/98-10
J
shNC
shHDAC10-2
shHDAC10-3
% input (LET7F2/98-9)
IgG
acetyl-H3-K9
acetyl-H3-K14
acetyl-H3-K18
acetyl-H3-K27
acetyl-H4-K5
shNC
shHDAC10-2
shHDAC10-3
anti-HDAC10
anti-tubulin
K
WT
KO
anti-Ack
anti-Ac-H3
anti-H3

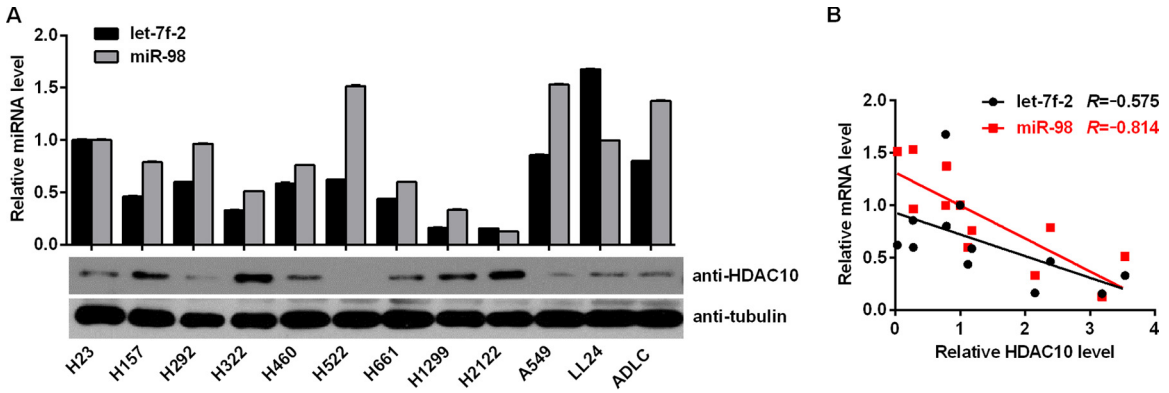

FIG 9 *let-7f-2* and miR-98 levels negatively correlate with *HDAC10* levels. (A) qPCR analysis of *let-7f-2* and miR-98 and Western blot analysis of HDAC10 in human NSCLC cell lines. (B) Relative miRNA levels plotted against HDAC10 levels.

HDACs might regulate HMGA2 expression. Exposure of cells to HDAC inhibitors reduced *HMGA2* transcription (44). HDAC1 and -2 repressed HMGA2 expression by regulating miR-23a, miR-26a, and miR-30a, which directly target *HMGA2* mRNA (45). We first examined whether HDAC10 regulated *HMGA2* at the transcriptional or posttranscriptional level and found that HDAC10 affected *HMGA2* mRNA stability (Fig. 8A) but not *HMGA2* promoter activity (Fig. 8B). *HMGA2* mRNA was more readily degraded in *HDAC10* knockdown cells than in control cells (Fig. 8A). A reporter assay showed that the *HMGA2* 3′ UTR was responsible for the reduction of *HMGA2* mRNA in *HDAC10* knockdown cells. 3′ UTR activity was decreased by *HDAC10* knockdown and increased by overexpression of ectopic HDAC10 (Fig. 8C). Collectively, these results indicated that HDAC10 positively regulates HMGA2 expression at the posttranscriptional level.

Many miRNAs directly target HMGA2 to regulate its expression. To validate whether these miRNAs were involved in HDAC10-mediated *HMGA2* 3′ UTR regulation, qPCR was used to detect the precursor forms of miRNAs that reportedly target HMGA2. Many *let-7* family members were highly expressed in *HDAC10* knockdown cells and reduced in cells overexpressing HDAC10 (Fig. 8D). The *HMGA2* 3′ UTR carries seven highly conserved *let-7* binding sites; *let-7* family members directly bind the 3′ UTR and negatively regulate its expression (37, 46, 47). Using luciferase reporter plasmids carrying the wild-type *HMGA2* 3′ UTR, transfection of cells with *let-7* and miR-98 repressed reporter activity. However, this effect was not seen with the UTR in which point mutations disrupted all seven *let-7* binding sites (Fig. 8E). Using the same reporter system, HDAC10 only regulated the wt HMGA2 3′ UTR, but not the mutant (Fig. 8C), which indicated that the effect of HDAC10 on the *HMGA2* 3′ UTR required some or all of the seven conserved *let-7* sites. We concluded that HDAC10 regulates the *HMGA2* 3′ UTR through *let-7* family members.

Among the *let-7* family members regulated by HDAC10, *let-7f-2* and miR-98 are located within the intron of the *HUWE1* gene on chromosome X, and both can be regulated by HDAC10 (Fig. 8D and G). Transcriptional regulation of *let-7f-2* and miR-98 is not well understood. Recent studies have reported that expression of these intragenic miRNAs is related to the host gene (48). Analysis of chromatin modification in the region surrounding these miRNAs suggested that transcription starts upstream of the host gene (48). In addition to sharing promoters with the protein-coding host genes, however, about 30% of intragenic miRNAs have their own transcriptional regulatory elements for independent expression from the intron (49, 50). A transcription start site (TSS) was predicted to be located upstream of *let-7f-2*/miR-98, within the intron (39, 48). Vitamin D receptor response elements (VDREs), which mediate regulation of miR-98 via 1α,25-dihydroxyvitamin D3 in LNCaP, are found in the 5′ region of miR-98 (39). To determine whether expression of *let-7f-2*/miR-98 and the host gene are both under the control of HDAC10, *HUWE1* expression levels in *HDAC10* knockdown and overexpressing cells were analyzed by qPCR. Results showed that the host gene was upregulated in HDAC10 knockdown cells and downregulated in HDAC10-overexpressing cells (Fig. 8F).

Next, ChIP was performed to map the HDAC10-binding region upstream of *let-7f-2*/miR-98 (Fig. 8G). Regions 1 to 7 were

FIG 8 HDAC10 represses *let-7f-2* and miR-98 transcription. (A) qPCR analysis of *HMGA2* mRNA stability in *HDAC10* knockdown (shHDAC10) and control (shGFP) H1299 cells at the indicated times after treatment with actinomycin D (AMD). *HMGA2* mRNA was normalized to rpL32 mRNA. (B) Results of the reporter assay for *HMGA2* promoter activity in *HDAC10* knockdown or overexpressing (HDAC10) cells and the respective control cells (shGFP and vector). (C) Reporter assay results with wild-type and mutant (-m7) *HMGA2* 3′ UTR in control (shNC) and *HDAC10* knockdown (shHDAC10), control (vector), and HDAC10-overexpressing (HDAC10) cells. (D) qPCR analysis of the change in expression of the indicated miRNAs in HDAC10-overexpressing and knockdown H1299 cells relative to their respective controls (defined as 1). (E) Results of reporter assay for the effect of HMGA2 wild-type (HMGA2-3UTR) and mutant (HMGA2-3UTR-m7) promoters on *let-7* and miR-98 expression. (F) qPCR analysis of *HUWE1* mRNA in *HDAC10* knockdown or overexpressing H1299 cells. (G) Schematic representation of locations of *let-7f-2* and miR-98 in the *HUWE1* intron on chromosome X. Numbered blocks indicate regions qPCR amplified after ChIP. (H, left) ChIP analysis results with *let-7f-2* and miR-98 promoter regions using anti-HDAC10 antibody or control IgG. (Right) Results of qPCR amplification of ChIP products, using anti-HDAC10 or control IgG and expressed as the percentage of the respective input. Values are means ± standard deviations. (I) Results of qPCR analysis after ChIP with anti-HDAC10 or control IgG of control and *HDAC10* knockdown H1299 cells. (J) ChIP results for comparison of acetylation status of the indicated histone residues in the *let-7f-2*/miR-98 promoter region in *HDAC10* knockdown and control cells. (K) Western analysis of histone acetylation. Core histones were purified from *HDAC10* wt and knockout MEFs by acid extraction. Acetylation of histone was detected by either anti-acetyl-lysine or anti-acetyl-histone H3 antibody. *, $P < 0.05$.

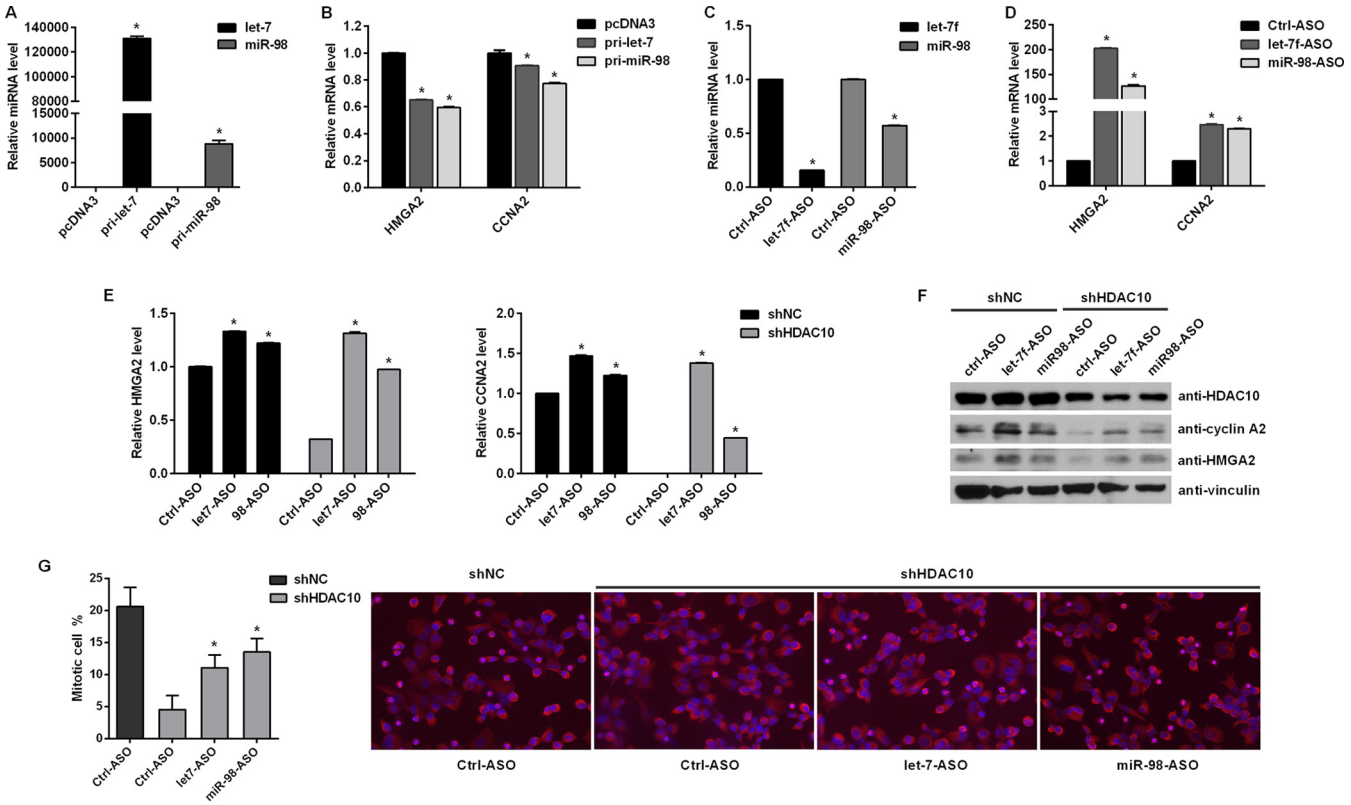

FIG 10 *let-7f* and miR-98 contribute to repression of *HMGA2* and cyclin A2 in *HDAC10* knockdown cells. (A and B) qPCR analysis of levels of miRNA (A) and HMGA2 and cyclin A2 mRNA (B) in H1299 cells transiently transfected with *let-7f* and miR-98 expression plasmids or control vector (pcDNA3). (C and D) qPCR analysis of levels of miRNA (C) and of HMGA2 and cyclin A2 mRNA (D) in H1299 cells treated with antisense oligonucleotides (ASOs) to block *let-7f* and miR-98 or control ASO. (E and F) qPCR analysis (E) of relative *HMGA2* (left) and cyclin A2 (*CCNA2*) (right) mRNA levels and Western analysis (F) of *HDAC10* knockdown (shHDAC10) and control (shNC) H1299 cells transfected with *let-7f* or miR-98 antisense oligonucleotides (ASOs). (G) Mitotic indices (left) and micrographs (right) of cells expressing the indicated shRNAs and transfected with *let-7f* or miR-98 ASOs, 40 min after release from RO-3306. Values are means ± standard deviations. *, $P < 0.05$.

identified as putative host gene promoter regions when we used Promoter Scan promoter prediction software, and regions 8 to 10 were the putative vitamin D receptor (VDR)-binding sites (39). ChIP analysis showed that HDAC10 binding was increased over a broad region upstream of *let-7f-2*/miR-98; however, no binding of HDAC10 was observed in the genomic region upstream of *let-7c*/miR-99a and miR-30a or to the cyclin A2 promoter region (Fig. 8H). HDAC10 enrichment at the *let-7f-2*/miR-98 promoter region decreased after *HDAC10* knockdown (Fig. 8I), which indicated the specificity of the interaction.

It has been reported that HDAC10 deacetylates histones *in vitro* and represses transcription when tethered to a target promoter (21–24). We validated the deacetylase activity of HDAC10 by Western blotting (Fig. 8K). To determine whether *let-7f-2*/miR-98 transcription was regulated by HDAC10-mediated histone modification, we carried out ChIP analysis and found that acetylation of histone H3 lysine 27 (H3K27), in the 5′ upstream/promoter region of *let-7f-2*/miR-98, was increased by 5- to 7-fold in *HDAC10* knockdown cells (Fig. 8J). There was also a modest increase in acetylation of H3K9, H3K14, and H3K18, but not of H4K5 (Fig. 8J). Therefore, HDAC10 may regulate *let-7-2* and miR-98 transcription via modification of promoter histone acetylation.

***let-7f-2* and miR-98 expression levels are negatively correlated with HDAC10 levels.** Because HDAC10 suppressed *let-7f-2*/miR-98 transcription, to determine whether an inverse relationship existed between HDAC10 and *let-7f-2*/miR-98 expression, HDAC10 expression was assessed by Western analysis, and *let-7f-2* and miR-98 expression was analyzed by qPCR in a panel of human NSCLC lines (Fig. 9A). Relative miRNA and HDAC10 expression levels in these cells lines were plotted against each other and showed a negative correlation coefficient (*R*) (Fig. 9B).

Blocking *let-7f* and miR-98 rescued HMGA2 and cyclin A2 repression in *HDAC10* knockdown cells. Many studies have suggested that *let-7* family members directly target and repress *HMGA2*. Our results indicated that overexpressing *let-7* and miR-98 reduced levels of *HMGA2* and cyclin A2 mRNA (Fig. 10A and B), whereas blocking *let-7* and miR-98 with antisense oligonucleotides increased these mRNA levels (Fig. 10C and D). This finding indicated that *let-7* family members might indirectly regulate cyclin A2 expression through HMGA2. Because HDAC10 suppressed *let-7f* and miR-98 transcription, if *let-7* family members were involved in HDAC10-mediated cyclin A2 regulation, then blocking *let-7f* and miR-98 with specific antisense oligonucleotides should abolish HMGA2 and cyclin A2 repression in *HDAC10* knockdown cells. qPCR and Western analysis showed that inhibition of *let-7f* and miR-98 partially abolished *HDAC10* knockdown-induced *HMGA2* and cyclin A2 repression (Fig. 10E and F) and partially rescued *HDAC10* knockdown-induced G_2/M

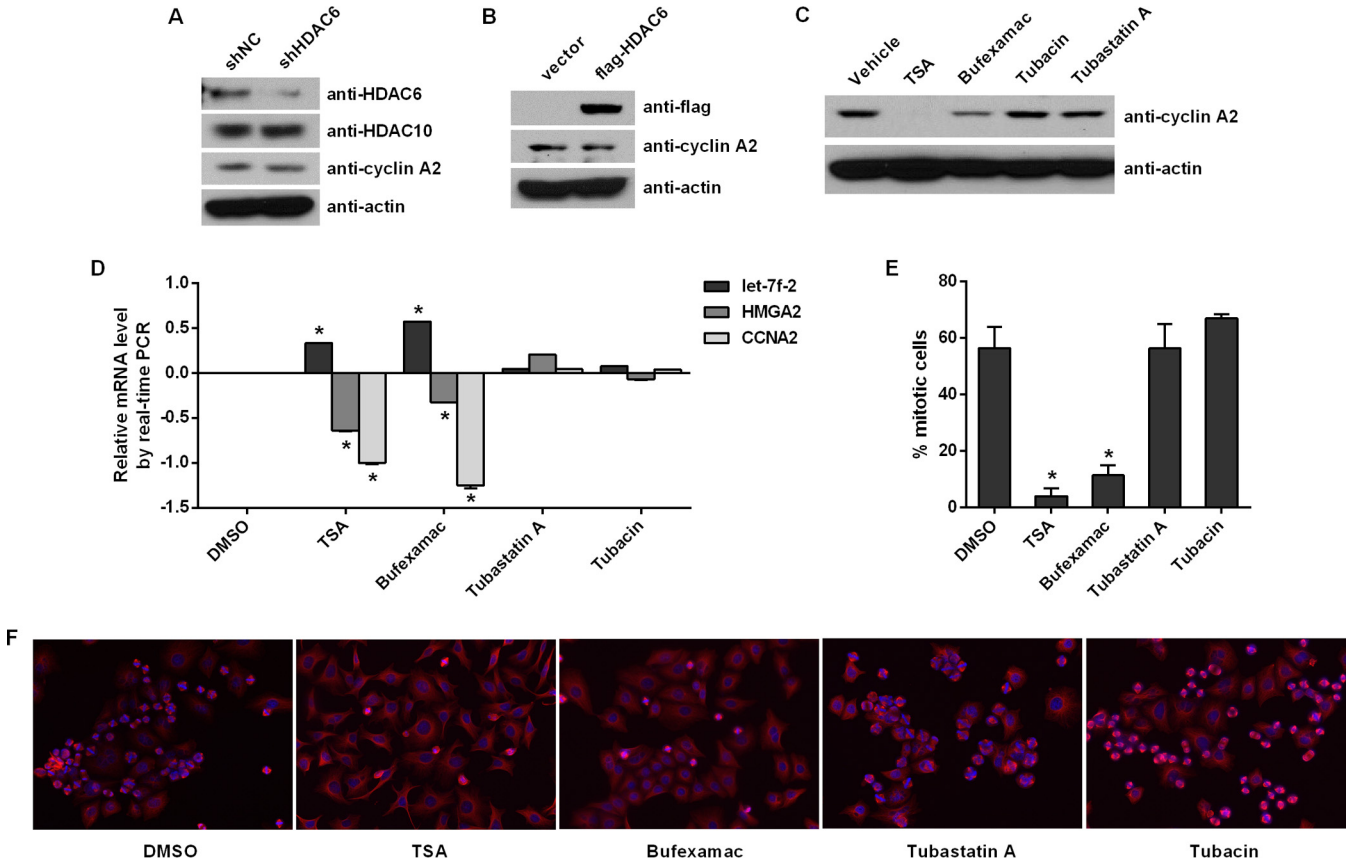

FIG 11 HDAC10, but not HDAC6, regulates the G_2/M transition via cyclin A2. (A and B) Western blot analysis results for cyclin A2 in H1299 cells 48 h after transient transfection with control vector or *HDAC6* knockdown (A) or overexpression (B) plasmid. (C) Western blot analysis of cyclin A2 in cells treated with 100 ng/ml TSA, 0.2 mM bufexamac, 0.5 μM tubastatin A, 2 μM tubacin, or solvent control for 24 h. (D) qPCR analysis of cyclin A2, *HMGA2*, and *let-7f-2* mRNA levels in H1299 cells treated with the indicated HDAC inhibitors or solvent control (as decribed for panel C) for 24 h. (E and F) Mitotic indices (E) and micrographs (F) of cells treated with the indicated HDAC inhibitors or solvent control together with 10 μM RO-3306 for 24 h, 40 min after release from RO-3306. Values represent means ± standard deviations. *, $P < 0.05$.

arrest (Fig. 10G). These findings indicated the important role of the *let-7* family in the HDAC10-related regulatory network.

HDAC10, but not HDAC6, regulates the G_2/M transition via cyclin A2. To study the specific effect of HDAC10 on cell cycle regulation, HDAC6, another class IIb HDAC member, was either overexpressed or depleted in H1299 cells. Western blot analysis showed that HDAC6 did not regulate the cyclin A2 level (Fig. 11A and B). It was reported that HDAC10 enzymatic activity is sensitive to TSA (21, 24), a pan-HDAC inhibitors, and class IIb inhibitor bufexamac (3). To further study the effect of HDAC10 inhibition on cyclin A2 expression, H1299 cells were treated with TSA and bufexamac, as well as the HDAC6-selective inhibitors tubacin and tubastatin A. Cyclin A2 mRNA and protein levels were both reduced by TSA and bufexamac treatment (Fig. 11C and D). TSA and bufexamac treatment also induced significant G_2/M arrest (Fig. 11E and F). However, treatment with the HDAC6-selective inhibitors tubacin and tubastatin A did not affect the cyclin A2 level (Fig. 11C and D) and did not cause G_2/M arrest after release from RO-3306 block (Fig. 11E and F), which indicated that these two class IIb HDAC family members have different functions in cell cycle regulation. Consistent with the idea that HDAC10 regulates cyclin A2 transcription through the let-7 and HMGA2 pathway, TSA and bufexamac treatment caused an increase in *let-7f-2* and a decrease in *HMGA2* mRNA levels (Fig. 11D). Treatment of cells with a class I enzyme inhibitor, such as MS-275, also induced a significant decrease in the cyclin A2 level (data not shown), but the mechanism by which MS-275 regulates cyclin A2 expression is still unknown.

DISCUSSION

The key components of the cell cycle machinery are the cyclin family of proteins and their associated CDKs. Complexes composed of various cyclin-CDK combinations regulate orderly progression through the cell cycle. Cyclin A was the first cyclin identified (51). Mammals express two A-type cyclins, embryonic-specific cyclin A1 and somatic cyclin A2. Because cyclin A1 expression is restricted to the testis, it primarily functions in the meiotic cell cycle. However, cyclin A2 is the major A-type cyclin in somatic cells (52). Cyclin A2 is ubiquitously expressed in proliferating cells and is essential for both the S and G_2/M phases of the cell cycle. It is required for activation and nuclear accumulation of the cyclin B/CDK1 complex and is the rate-limiting factor for completion of prophase (41, 42). Therefore, cyclin A2 knockdown causes a substantial delay in chromatin condensation and histone H3 phosphorylation, indicating impairment of mitotic entry. At late prophase, cyclin A2 may no longer be necessary as cyclin B/CDK1

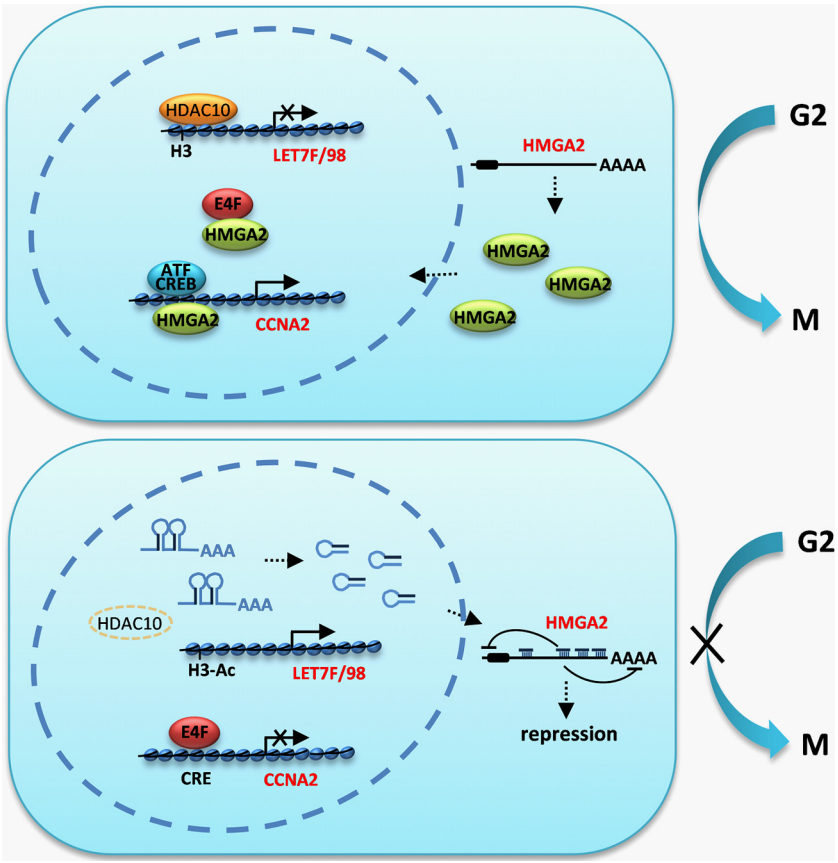

FIG 12 Proposed model of HDAC10 regulation in G_2/M transition. Under basal conditions, HDAC10 binds to the *let-7f-2*/miR-98 promoter region and deacetylates histone H3. *let-7* repression results in upregulation of HMGA2. HMGA2 interferes with E4F binding to the cyclin A2 promoter and activates cyclin A2 transcription. In *HDAC10* knockdown cells, expression levels of *let-7f* and miR-98, which mediate *HMGA2* mRNA degradation, increase. Loss of HMGA2 promotes E4F binding to the cyclin A2 promoter, inhibiting its transcription.

becomes active, so it is rapidly degraded by the anaphase-promoting complex/cyclosome (APC/C) via proteasomes (53, 54). Here, we showed that *HDAC10* knockdown impaired mitotic entry, and this G_2/M arrest was associated with loss of cyclin A2. Cyclin A2 expression was increased in HDAC10-overexpressing cells and decreased in *HDAC10* knockdown cells, and ectopic cyclin A2 rescued *HDAC10* knockdown-induced mitotic arrest. In a panel of NSCLC cell lines, the extent of mitotic arrest in *HDAC10* knockdown cells correlated with the degree of reduction of cyclin A2. These findings demonstrated that *HDAC10* knockdown-induced delay of entry into mitosis was due to loss of cyclin A2. HDAC10 did not bind to the cyclin A2 promoter but indirectly regulated promoter activity through the ATF/CRE binding site.

Comparative RNA sequence analysis confirmed that HMGA2, a member of the nonhistone chromosomal high-mobility group (HMG) protein family, was downregulated in *HDAC10* knockdown cells. HMG proteins modulate gene expression by altering chromatin architecture and/or recruiting other proteins to the transcription regulatory complex (55). HMGA2 is highly expressed in various undifferentiated tissues during embryonic development, and expression is also elevated in a variety of cancer cells, implying that HMGA2 plays a role in controlling proliferation and differentiation (56–58). Furthermore, HMGA2 was shown to activate the cyclin A2 promoter by counteracting the repressive activity of $p120^{E4F}$ via the ATF/CRE site (34). Our data showed that the effect of HDAC10 on the cyclin A2 promoter also was dependent on ATF/CRE binding sites. *HMGA2*-depleted cells exhibited a phenotype similar to that of *HDAC10* knockdown cells, i.e., proliferation was suppressed and mitotic entry after release from RO-3306 block in G_2 was inhibited. Therefore, we propose that the effect of HDAC10 on cyclin A2 regulation depends on HMGA2. A recent study reported that HMGA2 promoted lung cancer progression by acting as a competing endogenous RNA for the *let-7* family; HMGA2 promoted lung cancer cell transformation in a *let-7* site-dependent manner (59). To determine whether *HMGA2* operates both as a protein-coding gene and noncoding RNA for HDAC10-mediated cyclin A2 regulation, we performed a rescue assay by overexpressing the *HMGA2*-coding sequence without the 3′ UTR. HMGA2 overexpression in *HDAC10* knockdown cells partially abrogated transcriptional repression of endogenous cyclin A2. In *HDAC10* knockdown cells, reduced HMGA2 levels caused enrichment of the transcriptional repressor $p120^{E4F}$ at the cyclin A2 promoter, ultimately resulting in inhibition of cyclin A2 transcription. These findings demonstrated that *HMGA2* plays a key role in HDAC10-mediated cyclin A2 transcriptional regulation by operating as a protein-coding gene.

HMGA2 is the downstream target of the *let-7* family (37, 46, 47, 60). The human *let-7* family contains 13 members, including *let-7a-1*, *let-7a-2*, *let-7a-3*, *let-7b*, *let-7c*, *let-7d*, *let-7e*, *let-7f-1*, *let-7f-2*, *let-7g*, *let-7i*, miR-98, and miR-202 (61). Some members map

to genomic regions altered or deleted in human tumors (62), and some have been implicated as tumor suppressors, based on targeting of well-known oncogenes, such as the Ras family (63), *HMGA2* (47), c-Myc (64), and cell cycle regulators (65–67). *let-7* family members repress cell proliferation pathways, inhibit cell growth, and impair tumor development (65, 68). *let-7b* regulates melanoma cell growth by downregulating expression of cyclins D1, D3, and A and Cdk4 (69). In primary fibroblasts, *let-7b* or *let-7c* caused decreased proliferation and accumulation of cells in G_2/M. *let-7b* negatively regulates the E2 ubiquitin-conjugating enzyme Cdc34, which mediates proteolytic degradation of Wee1 kinase (70). *let-7a*, *let-7b*, *let-7e*, and *let-7f* were underexpressed in less differentiated $CD44^+$ PCa cells; *let-7* overexpression inhibited PCa cell proliferation and clonal expansion by inducing arrest in G_2/M phase (71). miR-98 was transcriptionally induced by vitamin D in LNCaP cells and contributed to the antiproliferative effect of vitamin D. miR-98 expression caused G_2/M arrest in LNCaP cells via downregulation of CCNJ (39). Here, qPCR analysis showed that HDAC10 suppressed *let-7f-2* and miR-98 transcription. HDAC10 bound to the *let-7f-2*/miR-98 promoter region and mediated histone H3K27 deacetylation. Blocking *let-7f* and miR-98 in *HDAC10* knockdown cells rescued repression of *HMGA2* and cyclin A2 and partially abolished *HDAC10* knockdown-induced G_2/M arrest, which demonstrated that HDAC10 and its downstream *let-7/HMGA2*/cyclin A2 axis are required for the growth of lung cancer cells.

In summary, we showed that HDAC10 regulates G_2/M transition via a novel pathway that involves *let-7/HMGA2*/cyclin A2 (Fig. 12). HDAC10 deacetylated histone H3 surrounding the *let-7f-2*/miR-98 promoter and repressed transcription. Loss of *let-7* family members contributed to increased HMGA2 expression. HMGA2 interfered with E4F binding to the ATF/CRE site in the cyclin A2 promoter and facilitated binding of ATF and CREB family members, which resulted in activation of cyclin A2 transcription. When *HDAC10* was knocked down, the *let-7f-2*/miR-98 promoter was activated by histone H3 acetylation. *let-7f* and miR-98 expression levels increased, which directly target the *HMGA2* mRNA 3′ UTR and mediate its degradation. Decreased HMGA2 expression resulted in enrichment of E4F at the cyclin A2 promoter, which inhibited its transcription. Finally, loss of cyclin A2 contributed to inhibition of the G_2/M transition. Together, these findings provide novel insights into the mechanism of HDAC10 in cell cycle regulation and will allow us to further study and develop approaches to target HDAC10 in diseases associated with abnormal HDAC10 expression and a dysregulated cell cycle.

ACKNOWLEDGMENTS

This work was supported by grants to E.S. from the National Institutes of Health and the Kaul Foundation.

Y.L. and E.S. conceived the project; Y.L. performed most of the experiments, with support and help from L.P.; Y.L. and E.S. wrote the manuscript with input from L.P.

We thank Thomas Rosahl at Merck & Co., Inc., for the *Hdac10*$^{tm1.2Mrl}$ constitutive knockout mouse line, which was generated at the Institut Clinique de la Souris (ICS; llkirch, France) in collaboration with Merck & Co., Inc., and can be obtained via Taconic through nonprofit organizations. We also thank the Moffitt Cancer Center Core Facility for technical support and Mark Alexandrow, Doug Cress, and Jia Fang for discussion and critical reading of the manuscript.

We declare no conflicts of interest.

REFERENCES

1. **Yang XJ, Seto E.** 2008. Lysine acetylation: codified crosstalk with other posttranslational modifications. Mol Cell **31:**449–461. http://dx.doi.org/10.1016/j.molcel.2008.07.002.
2. **Sengupta N, Seto E.** 2004. Regulation of histone deacetylase activities. J Cell Biochem **93:**57–67. http://dx.doi.org/10.1002/jcb.20179.
3. **Bantscheff M, Hopf C, Savitski MM, Dittmann A, Grandi P, Michon AM, Schlegl J, Abraham Y, Becher I, Bergamini G, Boesche M, Delling M, Dumpelfeld B, Eberhard D, Huthmacher C, Mathieson T, Poeckel D, Reader V, Strunk K, Sweetman G, Kruse U, Neubauer G, Ramsden NG, Drewes G.** 2011. Chemoproteomics profiling of HDAC inhibitors reveals selective targeting of HDAC complexes. Nat Biotechnol **29:**255–265. http://dx.doi.org/10.1038/nbt.1759.
4. **Haggarty SJ, Koeller KM, Wong JC, Grozinger CM, Schreiber SL.** 2003. Domain-selective small-molecule inhibitor of histone deacetylase 6 (HDAC6)-mediated tubulin deacetylation. Proc Natl Acad Sci U S A **100:**4389–4394. http://dx.doi.org/10.1073/pnas.0430973100.
5. **Butler KV, Kalin J, Brochier C, Vistoli G, Langley B, Kozikowski AP.** 2010. Rational design and simple chemistry yield a superior, neuroprotective HDAC6 inhibitor, tubastatin A. J Am Chem Soc **132:**10842–10846. http://dx.doi.org/10.1021/ja102758v.
6. **Scholz C, Weinert BT, Wagner SA, Beli P, Miyake Y, Qi J, Jensen LJ, Streicher W, McCarthy AR, Westwood NJ, Lain S, Cox J, Matthias P, Mann M, Bradner JE, Choudhary C.** 2015. Acetylation site specificities of lysine deacetylase inhibitors in human cells. Nat Biotechnol **33:**415–423. http://dx.doi.org/10.1038/nbt.3130.
7. **Glaser KB, Li J, Staver MJ, Wei RQ, Albert DH, Davidsen SK.** 2003. Role of class I and class II histone deacetylases in carcinoma cells using siRNA. Biochem Biophys Res Commun **310:**529–536. http://dx.doi.org/10.1016/j.bbrc.2003.09.043.
8. **Finzer P, Kuntzen C, Soto U, zur Hausen H, Rosl F.** 2001. Inhibitors of histone deacetylase arrest cell cycle and induce apoptosis in cervical carcinoma cells circumventing human papillomavirus oncogene expression. Oncogene **20:**4768–4776. http://dx.doi.org/10.1038/sj.onc.1204652.
9. **Reichert N, Choukrallah MA, Matthias P.** 2012. Multiple roles of class I HDACs in proliferation, differentiation, and development. Cell Mol Life Sci **69:**2173–2187. http://dx.doi.org/10.1007/s00018-012-0921-9.
10. **Lagger G, O'Carroll D, Rembold M, Khier H, Tischler J, Weitzer G, Schuettengruber B, Hauser C, Brunmeir R, Jenuwein T, Seiser C.** 2002. Essential function of histone deacetylase 1 in proliferation control and CDK inhibitor repression. EMBO J **21:**2672–2681. http://dx.doi.org/10.1093/emboj/21.11.2672.
11. **Zupkovitz G, Grausenburger R, Brunmeir R, Senese S, Tischler J, Jurkin J, Rembold M, Meunier D, Egger G, Lagger S, Chiocca S, Propst F, Weitzer G, Seiser C.** 2010. The cyclin-dependent kinase inhibitor p21 is a crucial target for histone deacetylase 1 as a regulator of cellular proliferation. Mol Cell Biol **30:**1171–1181. http://dx.doi.org/10.1128/MCB.01500-09.
12. **Yamaguchi T, Cubizolles F, Zhang Y, Reichert N, Kohler H, Seiser C, Matthias P.** 2010. Histone deacetylases 1 and 2 act in concert to promote the G_1-to-S progression. Genes Dev **24:**455–469. http://dx.doi.org/10.1101/gad.552310.
13. **Senese S, Zaragoza K, Minardi S, Muradore I, Ronzoni S, Passafaro A, Bernard L, Draetta GF, Alcalay M, Seiser C, Chiocca S.** 2007. Role for histone deacetylase 1 in human tumor cell proliferation. Mol Cell Biol **27:**4784–4795. http://dx.doi.org/10.1128/MCB.00494-07.
14. **Blagosklonny MV, Robey R, Sackett DL, Du L, Traganos F, Darzynkiewicz Z, Fojo T, Bates SE.** 2002. Histone deacetylase inhibitors all induce p21 but differentially cause tubulin acetylation, mitotic arrest, and cytotoxicity. Mol Cancer Ther **1:**937–941.
15. **Donadelli M, Costanzo C, Faggioli L, Scupoli MT, Moore PS, Bassi C, Scarpa A, Palmieri M.** 2003. Trichostatin A, an inhibitor of histone deacetylases, strongly suppresses growth of pancreatic adenocarcinoma cells. Mol Carcinog **38:**59–69. http://dx.doi.org/10.1002/mc.10145.
16. **Noh EJ, Lee JS.** 2003. Functional interplay between modulation of histone deacetylase activity and its regulatory role in G_2-M transition. Biochem Biophys Res Commun **310:**267–273. http://dx.doi.org/10.1016/j.bbrc.2003.09.013.
17. **Atadja P, Gao L, Kwon P, Trogani N, Walker H, Hsu M, Yeleswarapu L, Chandramouli N, Perez L, Versace R, Wu A, Sambucetti L, Lassota P, Cohen D, Bair K, Wood A, Remiszewski S.** 2004. Selective growth inhibition of tumor cells by a novel histone deacetylase inhibitor, NVP-LAQ824. Cancer Res **64:**689–695. http://dx.doi.org/10.1158/0008-5472.CAN-03-2043.

18. **Takai N, Desmond JC, Kumagai T, Gui D, Said JW, Whittaker S, Miyakawa I, Koeffler HP.** 2004. Histone deacetylase inhibitors have a profound antigrowth activity in endometrial cancer cells. Clin Cancer Res **10:**1141–1149. http://dx.doi.org/10.1158/1078-0432.CCR-03-0100.
19. **Li Y, Kao GD, Garcia BA, Shabanowitz J, Hunt DF, Qin J, Phelan C, Lazar MA.** 2006. A novel histone deacetylase pathway regulates mitosis by modulating Aurora B kinase activity. Genes Dev **20:**2566–2579. http://dx.doi.org/10.1101/gad.1455006.
20. **Vidal-Laliena M, Gallastegui E, Mateo F, Martinez-Balbas M, Pujol MJ, Bachs O.** 2013. Histone deacetylase 3 regulates cyclin A stability. J Biol Chem **288:**21096–21104. http://dx.doi.org/10.1074/jbc.M113.458323.
21. **Tong JJ, Liu J, Bertos NR, Yang XJ.** 2002. Identification of HDAC10, a novel class II human histone deacetylase containing a leucine-rich domain. Nucleic Acids Res **30:**1114–1123. http://dx.doi.org/10.1093/nar/30.5.1114.
22. **Guardiola AR, Yao TP.** 2002. Molecular cloning and characterization of a novel histone deacetylase HDAC10. J Biol Chem **277:**3350–3356. http://dx.doi.org/10.1074/jbc.M109861200.
23. **Kao HY, Lee CH, Komarov A, Han CC, Evans RM.** 2002. Isolation and characterization of mammalian HDAC10, a novel histone deacetylase. J Biol Chem **277:**187–193. http://dx.doi.org/10.1074/jbc.M108931200.
24. **Fischer DD, Cai R, Bhatia U, Asselbergs FA, Song C, Terry R, Trogani N, Widmer R, Atadja P, Cohen D.** 2002. Isolation and characterization of a novel class II histone deacetylase, HDAC10. J Biol Chem **277:**6656–6666. http://dx.doi.org/10.1074/jbc.M108055200.
25. **Lee JH, Jeong EG, Choi MC, Kim SH, Park JH, Song SH, Park J, Bang YJ, Kim TY.** 2010. Inhibition of histone deacetylase 10 induces thioredoxin-interacting protein and causes accumulation of reactive oxygen species in SNU-620 human gastric cancer cells. Mol Cells **30:**107–112. http://dx.doi.org/10.1007/s10059-010-0094-z.
26. **Song C, Zhu S, Wu C, Kang J.** 2013. Histone deacetylase (HDAC) 10 suppresses cervical cancer metastasis through inhibition of matrix metalloproteinase (MMP) 2 and 9 expression. J Biol Chem **288:**28021–28033. http://dx.doi.org/10.1074/jbc.M113.498758.
27. **Shimazu T, Horinouchi S, Yoshida M.** 2007. Multiple histone deacetylases and the CREB-binding protein regulate pre-mRNA 3′-end processing. J Biol Chem **282:**4470–4478. http://dx.doi.org/10.1074/jbc.M609745200.
28. **Oehme I, Linke JP, Bock BC, Milde T, Lodrini M, Hartenstein B, Wiegand I, Eckert C, Roth W, Kool M, Kaden S, Grone HJ, Schulte JH, Lindner S, Hamacher-Brady A, Brady NR, Deubzer HE, Witt O.** 2013. Histone deacetylase 10 promotes autophagy-mediated cell survival. Proc Natl Acad Sci U S A **110:**E2592–E2601. http://dx.doi.org/10.1073/pnas.1300113110.
29. **Osada H, Tatematsu Y, Saito H, Yatabe Y, Mitsudomi T, Takahashi T.** 2004. Reduced expression of class II histone deacetylase genes is associated with poor prognosis in lung cancer patients. Int J Cancer **112:**26–32. http://dx.doi.org/10.1002/ijc.20395.
30. **Fonseca AL, Kugelberg J, Starker LF, Scholl U, Choi M, Hellman P, Akerstrom G, Westin G, Lifton RP, Bjorklund P, Carling T.** 2012. Comprehensive DNA methylation analysis of benign and malignant adrenocortical tumors. Genes Chromosomes Cancer **51:**949–960. http://dx.doi.org/10.1002/gcc.21978.
31. **Jin Z, Jiang W, Jiao F, Guo Z, Hu H, Wang L, Wang L.** 2014. Decreased expression of histone deacetylase 10 predicts poor prognosis of gastric cancer patients. Int J Clin Exp Pathol **7:**5872–5879.
32. **Wang JC, Kafeel MI, Avezbakiyev B, Chen C, Sun Y, Rathnasabapathy C, Kalavar M, He Z, Burton J, Lichter S.** 2011. Histone deacetylase in chronic lymphocytic leukemia. Oncology **81:**325–329. http://dx.doi.org/10.1159/000334577.
33. **Jozefczuk J, Drews K, Adjaye J.** 2012. Preparation of mouse embryonic fibroblast cells suitable for culturing human embryonic and induced pluripotent stem cells. J Vis Exp **64:**pii=38854. http://dx.doi.org/10.3791/3854.
34. **Tessari MA, Gostissa M, Altamura S, Sgarra R, Rustighi A, Salvagno C, Caretti G, Imbriano C, Mantovani R, Del Sal G, Giancotti V, Manfioletti G.** 2003. Transcriptional activation of the cyclin A gene by the architectural transcription factor HMGA2. Mol Cell Biol **23:**9104–9116. http://dx.doi.org/10.1128/MCB.23.24.9104-9116.2003.
35. **Nakamura Y, Igarashi K, Suzuki T, Kanno J, Inoue T, Tazawa C, Saruta M, Ando T, Moriyama N, Furukawa T, Ono M, Moriya T, Ito K, Saito H, Ishibashi T, Takahashi S, Yamada S, Sasano H.** 2004. E4F1, a novel estrogen-responsive gene in possible atheroprotection, revealed by microarray analysis. Am J Pathol **165:**2019–2031. http://dx.doi.org/10.1016/S0002-9440(10)63253-1.
36. **Vassilev LT.** 2006. Cell cycle synchronization at the G_2/M phase border by reversible inhibition of CDK1. Cell Cycle **5:**2555–2556. http://dx.doi.org/10.4161/cc.5.22.3463.
37. **Mayr C, Hemann MT, Bartel DP.** 2007. Disrupting the pairing between let-7 and Hmga2 enhances oncogenic transformation. Science **315:**1576–1579. http://dx.doi.org/10.1126/science.1137999.
38. **Villagra A, Ulloa N, Zhang X, Yuan Z, Sotomayor E, Seto E.** 2007. Histone deacetylase 3 down-regulates cholesterol synthesis through repression of lanosterol synthase gene expression. J Biol Chem **282:**35457–35470. http://dx.doi.org/10.1074/jbc.M701719200.
39. **Ting HJ, Messing J, Yasmin-Karim S, Lee YF.** 2013. Identification of microRNA-98 as a therapeutic target inhibiting prostate cancer growth and a biomarker induced by vitamin D. J Biol Chem **288:**1–9. http://dx.doi.org/10.1074/jbc.M112.395947.
40. **Pelosi A, Careccia S, Sagrestani G, Nanni S, Manni I, Schinzari V, Martens JH, Farsetti A, Stunnenberg HG, Gentileschi MP, Del Bufalo D, De Maria R, Piaggio G, Rizzo MG.** 2014. Dual promoter usage as regulatory mechanism of let-7c expression in leukemic and solid tumors. Mol Cancer Res **12:**878–889. http://dx.doi.org/10.1158/1541-7786.MCR-13-0410.
41. **Gong D, Ferrell JE, Jr.** 2010. The roles of cyclin A2, B1, and B2 in early and late mitotic events. Mol Biol Cell **21:**3149–3161. http://dx.doi.org/10.1091/mbc.E10-05-0393.
42. **Hochegger H, Takeda S, Hunt T.** 2008. Cyclin-dependent kinases and cell-cycle transitions: does one fit all? Nat Rev Mol Cell Biol **9:**910–916. http://dx.doi.org/10.1038/nrm2510.
43. **Fung TK, Ma HT, Poon RY.** 2007. Specialized roles of the two mitotic cyclins in somatic cells: cyclin A as an activator of M phase-promoting factor. Mol Biol Cell **18:**1861–1873. http://dx.doi.org/10.1091/mbc.E06-12-1092.
44. **Ferguson M, Henry PA, Currie RA.** 2003. Histone deacetylase inhibition is associated with transcriptional repression of the Hmga2 gene. Nucleic Acids Res **31:**3123–3133. http://dx.doi.org/10.1093/nar/gkg403.
45. **Lee S, Jung JW, Park SB, Roh K, Lee SY, Kim JH, Kang SK, Kang KS.** 2011. Histone deacetylase regulates high mobility group A2-targeting microRNAs in human cord blood-derived multipotent stem cell aging. Cell Mol Life Sci **68:**325–336. http://dx.doi.org/10.1007/s00018-010-0457-9.
46. **Hebert C, Norris K, Scheper MA, Nikitakis N, Sauk JJ.** 2007. High mobility group A2 is a target for miRNA-98 in head and neck squamous cell carcinoma. Mol Cancer **6:**5. http://dx.doi.org/10.1186/1476-4598-6-5.
47. **Lee YS, Dutta A.** 2007. The tumor suppressor microRNA let-7 represses the HMGA2 oncogene. Genes Dev **21:**1025–1030. http://dx.doi.org/10.1101/gad.1540407.
48. **Barski A, Jothi R, Cuddapah S, Cui K, Roh TY, Schones DE, Zhao K.** 2009. Chromatin poises miRNA- and protein-coding genes for expression. Genome Res **19:**1742–1751. http://dx.doi.org/10.1101/gr.090951.109.
49. **Ozsolak F, Poling LL, Wang Z, Liu H, Liu XS, Roeder RG, Zhang X, Song JS, Fisher DE.** 2008. Chromatin structure analyses identify miRNA promoters. Genes Dev **22:**3172–3183. http://dx.doi.org/10.1101/gad.1706508.
50. **Monteys AM, Spengler RM, Wan J, Tecedor L, Lennox KA, Xing Y, Davidson BL.** 2010. Structure and activity of putative intronic miRNA promoters. RNA **16:**495–505. http://dx.doi.org/10.1261/rna.1731910.
51. **Evans T, Rosenthal ET, Youngblom J, Distel D, Hunt T.** 1983. Cyclin: a protein specified by maternal mRNA in sea urchin eggs that is destroyed at each cleavage division. Cell **33:**389–396. http://dx.doi.org/10.1016/0092-8674(83)90420-8.
52. **Nieduszynski CA, Murray J, Carrington M.** 2002. Whole-genome analysis of animal A- and B-type cyclins. Genome Biol **3:**RESEARCH0070.
53. **den Elzen N, Pines J.** 2001. Cyclin A is destroyed in prometaphase and can delay chromosome alignment and anaphase. J Cell Biol **153:**121–136. http://dx.doi.org/10.1083/jcb.153.1.121.
54. **Geley S, Kramer E, Gieffers C, Gannon J, Peters JM, Hunt T.** 2001. Anaphase-promoting complex/cyclosome-dependent proteolysis of human cyclin A starts at the beginning of mitosis and is not subject to the spindle assembly checkpoint. J Cell Biol **153:**137–148. http://dx.doi.org/10.1083/jcb.153.1.137.
55. **Pfannkuche K, Summer H, Li O, Hescheler J, Droge P.** 2009. The high mobility group protein HMGA2: a co-regulator of chromatin structure and pluripotency in stem cells? Stem Cell Rev **5:**224–230. http://dx.doi.org/10.1007/s12015-009-9078-9.
56. **Ashar HR, Chouinard RA, Jr, Dokur M, Chada K.** 2010. In vivo mod-

ulation of HMGA2 expression. Biochim Biophys Acta **1799:**55–61. http://dx.doi.org/10.1016/j.bbagrm.2009.11.013.

57. **Li Z, Gilbert JA, Zhang Y, Zhang M, Qiu Q, Ramanujan K, Shavlakadze T, Eash JK, Scaramozza A, Goddeeris MM, Kirsch DG, Campbell KP, Brack AS, Glass DJ.** 2012. An HMGA2-IGF2BP2 axis regulates myoblast proliferation and myogenesis. Dev Cell **23:**1176–1188. http://dx.doi.org/10.1016/j.devcel.2012.10.019.
58. **Yu KR, Park SB, Jung JW, Seo MS, Hong IS, Kim HS, Seo Y, Kang TW, Lee JY, Kurtz A, Kang KS.** 2013. HMGA2 regulates the in vitro aging and proliferation of human umbilical cord blood-derived stromal cells through the mTOR/p70S6K signaling pathway. Stem Cell Res **10:**156–165. http://dx.doi.org/10.1016/j.scr.2012.11.002.
59. **Kumar MS, Armenteros-Monterroso E, East P, Chakravorty P, Matthews N, Winslow MM, Downward J.** 2014. HMGA2 functions as a competing endogenous RNA to promote lung cancer progression. Nature **505:**212–217. http://dx.doi.org/10.1038/nature12785.
60. **Park SM, Shell S, Radjabi AR, Schickel R, Feig C, Boyerinas B, Dinulescu DM, Lengyel E, Peter ME.** 2007. Let-7 prevents early cancer progression by suppressing expression of the embryonic gene HMGA2. Cell Cycle **6:**2585–2590. http://dx.doi.org/10.4161/cc.6.21.4845.
61. **Roush S, Slack FJ.** 2008. The let-7 family of microRNAs. Trends Cell Biol **18:**505–516. http://dx.doi.org/10.1016/j.tcb.2008.07.007.
62. **Calin GA, Sevignani C, Dumitru CD, Hyslop T, Noch E, Yendamuri S, Shimizu M, Rattan S, Bullrich F, Negrini M, Croce CM.** 2004. Human microRNA genes are frequently located at fragile sites and genomic regions involved in cancers. Proc Natl Acad Sci U S A **101:**2999–3004. http://dx.doi.org/10.1073/pnas.0307323101.
63. **Johnson SM, Grosshans H, Shingara J, Byrom M, Jarvis R, Cheng A, Labourier E, Reinert KL, Brown D, Slack FJ.** 2005. RAS is regulated by the let-7 microRNA family. Cell **120:**635–647. http://dx.doi.org/10.1016/j.cell.2005.01.014.
64. **Kumar MS, Lu J, Mercer KL, Golub TR, Jacks T.** 2007. Impaired microRNA processing enhances cellular transformation and tumorigenesis. Nat Genet **39:**673–677. http://dx.doi.org/10.1038/ng2003.
65. **Johnson CD, Esquela-Kerscher A, Stefani G, Byrom M, Kelnar K, Ovcharenko D, Wilson M, Wang X, Shelton J, Shingara J, Chin L, Brown D, Slack FJ.** 2007. The let-7 microRNA represses cell proliferation pathways in human cells. Cancer Res **67:**7713–7722. http://dx.doi.org/10.1158/0008-5472.CAN-07-1083.
66. **Zhao C, Sun G, Li S, Lang MF, Yang S, Li W, Shi Y.** 2010. MicroRNA let-7b regulates neural stem cell proliferation and differentiation by targeting nuclear receptor TLX signaling. Proc Natl Acad Sci U S A **107:**1876–1881. http://dx.doi.org/10.1073/pnas.0908750107.
67. **Mitra D, Das PM, Huynh FC, Jones FE.** 2011. Jumonji/ARID1 B (JARID1B) protein promotes breast tumor cell cycle progression through epigenetic repression of microRNA let-7e. J Biol Chem **286:**40531–40535. http://dx.doi.org/10.1074/jbc.M111.304865.
68. **Kumar MS, Erkeland SJ, Pester RE, Chen CY, Ebert MS, Sharp PA, Jacks T.** 2008. Suppression of non-small cell lung tumor development by the let-7 microRNA family. Proc Natl Acad Sci U S A **105:**3903–3908. http://dx.doi.org/10.1073/pnas.0712321105.
69. **Schultz J, Lorenz P, Gross G, Ibrahim S, Kunz M.** 2008. MicroRNA let-7b targets important cell cycle molecules in malignant melanoma cells and interferes with anchorage-independent growth. Cell Res **18:**549–557. http://dx.doi.org/10.1038/cr.2008.45.
70. **Legesse-Miller A, Elemento O, Pfau SJ, Forman JJ, Tavazoie S, Coller HA.** 2009. let-7 overexpression leads to an increased fraction of cells in G_2/M, direct down-regulation of Cdc34, and stabilization of Wee1 kinase in primary fibroblasts. J Biol Chem **284:**6605–6609. http://dx.doi.org/10.1074/jbc.C900002200.
71. **Liu C, Kelnar K, Vlassov AV, Brown D, Wang J, Tang DG.** 2012. Distinct microRNA expression profiles in prostate cancer stem/progenitor cells and tumor-suppressive functions of let-7. Cancer Res **72:**3393–3404. http://dx.doi.org/10.1158/0008-5472.CAN-11-3864.